國立臺灣大學工學院機械工程學系

碩士論文

Department of Mechanical Engineering
College of Engineering
National Taiwan University
Master's Thesis

針對混合乾羽毛於液體中分選收集之流場開發

Liquid channel development for separation and collection of dry feather mixtures in aqueous environment

賴以軒

Yi-Hsuan Lai

指導教授：楊馥菱 博士

Advisor: Fu-Ling Yang, Ph.D.

中華民國 113 年 7 月

July, 2024

doi:10.6342/NTU202404295

致謝

能完成這篇論文，我首先要特別感謝我的指導教授楊馥菱老師，謝謝老師兩年來的教導，以及最後花費了相當大的精神幫我修正論文。也要感謝實驗室從碩一修課到碩二研究，一路上互相支持的維軒和子震，以及哲鋒、祐瑜、志英、章奇、慕堯、宜修、建宏、雲陽、晨毓、晨誠學長姐們和立瑜、啟宣、鈞羿學弟們不時的指導討論及關照。最後謝謝所有我的家人、朋友們讓我遇到瓶頸時能無後顧之憂地專注在研究上，謝謝大家。

doi:10.6342/NTU202404295

中文摘要

本論文旨在設計一浸潤式流場分選系統將乾燥混合羽毛組成中的大尺寸毛片篩出，藉此提高羽絨於混合羽毛中之佔比。系統所使用之工作流體透過溶入特定濃度之氯化鈉以提升流體密度，進而強化浮力作用於不同種類羽毛的差異性以創造分離機制；同時，工作流體中也混入一定比例之介面活性劑，使之擁有可快速潤濕乾燥混合羽毛的特性，有助羽毛保持沉浸狀態。爾後我們設計一流場設備以配合工作流體特性來達到對乾燥混和樣本羽毛進行潤濕、疏鬆、運輸、分離以及收集等連續製程。此設備以一透明玻璃水缸盛裝工作流體，內部設置本論文設計並製作的特殊流道，經幫浦驅動水流後創造不同的工作流域並產生流場結構，透過流體動力及浮力耦合作用分選毛片及羽絨。本論文描述了設備發展過程中所出現的羽毛運動現象以及對應的設計抉擇，並予以工作機制之說明，更藉由實驗檢驗最終設計之有效性，若以同一種類羽毛的初始個數及分選後之個數百分比來評估分選效果，我們發現大尺寸毛片有 77%被成功篩出，而羽絨則有 87%被成功收集。我們更進一步比較改變流場設置對不同種類羽毛分選結果之影響，以討論相應的潛在控制參數。

關鍵字: 乾羽毛分選、流場設計、乾羽毛潤濕、羽毛解結、浮力分離

doi:10.6342/NTU202404295

ABSTRACT

In this study, an aqueous sorting system has been developed to sort out big feathers from a dry feather mixture, thereby increasing the proportion of downs in the output feather collection. The density of the working fluid is increased by dissolving a specific concentration of sodium chloride, thereby promoting the buoyancy-induced segregation effect on various types of feathers. Additionally, a certain concentration of surfactant is mixed into the working fluid to enable the wettability of the working fluid, with which we may promote the immersion state of the dry feather mixtures. Exploiting the unique properties of the working fluid, a flow facility is designed to achieve a continuous sorting process that includes wetting, disengaging, transporting, segregating, and collecting steps. The flow is driven a pump and moves through various flow channels in specific shapes and dimension, thereby creating specific flow fields or structures to meet the respective e functions in the process. The dynamics of feathers during the development of the apparatus are described with the flow physics and the working mechanisms and how they led to the design decisions. Through experimental validation, the effectiveness of the final design was evaluated by the number percentage of each type of feathers before and after the sorting process. We found that that 77% of the big feathers is successfully sorted out, while 87% of the down is successfully collected.

doi:10.6342/NTU202404295

Furthermore, the crucial flow design aspect is identified and investigated its effects on the sorting effectiveness to discuss the potential control parameters for further process enhancement.

Key words: sorting of dry feather mixtures, flow field design, wetting of dry feathers, feather detangling, buoyancy-induced segregation,

doi:10.6342/NTU202404295

Nomenclature

D	Down
BF	Big feather
SF	Small feather
η	Number ratio
$wt\%_s$	Weight percentage concentration of surfactant

doi:10.6342/NTU202404295

CONTENTS

doi:10.6342/NTU202404295

doi:10.6342/NTU202404295

LIST OF FIGURES

doi:10.6342/NTU202404295

doi:10.6342/NTU202404295

doi:10.6342/NTU202404295

doi:10.6342/NTU202404295

doi:10.6342/NTU202404295

doi:10.6342/NTU202404295

LIST OF TABLES

doi:10.6342/NTU202404295

Chapter 1 Introduction

Birds have various types of feathers on different parts of their bodies, each serving a unique function. Figure 1.1 illustrates the categories of feathers based on their structure and location on the bird. Among these categories, “down” refers to a layer of fine feathers found beneath the bird's tougher exterior feathers. Their loose, three-dimensional spherical structure enables them to trap a significant amount of air, forming an insulate on layer. Their loose, three-dimensional spherical structure enables them to trap a large amount of air, forming an insulating layer. Additionally, down is known for its extraordinary suppleness and flexibility. Nowadays, down is regarded as a premium insulation material in clothing and bedding, as compared to synthetic fibers.

Figure 1.1: Family of various feathers from a bird [1].

doi:10.6342/NTU202404295

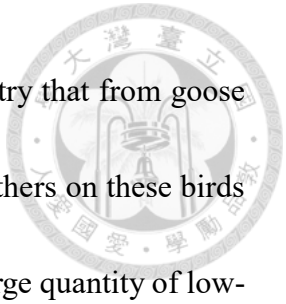

However, the primary source of downs used in the textile industry that from goose and duck, account for only 8 to 12 weight percentage of the total feathers on these birds [2]. What makes things worse is that downs are often mixed with a large quantity of low-insulating but water-repellent exterior feathers during the collection process. These factors combine to make down a natural material of high value.

In feather industry, dry feather mixtures first go through a series of sterilization and raw washing step, as shown in Figure 1.2 (a). Subsequently, to sort out the most valuable down feathers from other feathers, the feather mixture is made to fly through a series of vertical air sorting channels, as shown in Figure 1.2 (b). Feathers of varied weights and shapes are transported by airflow to varying distances and then sorted into sequential collection areas within these air channels. After sorting, the feathers undergo further processes including fine washing, sterilization, and drying before being packaged and sold.

The conventional sorting facility is designed to handle tons of mixed feathers simultaneously and is often as large as a three-story house. As a result, the sorting results of individual feathers of milligrams is prone to uncertainties due to differences in feather properties among sample batches. Hence, a refined sorting process is desired.

doi:10.6342/NTU202404295

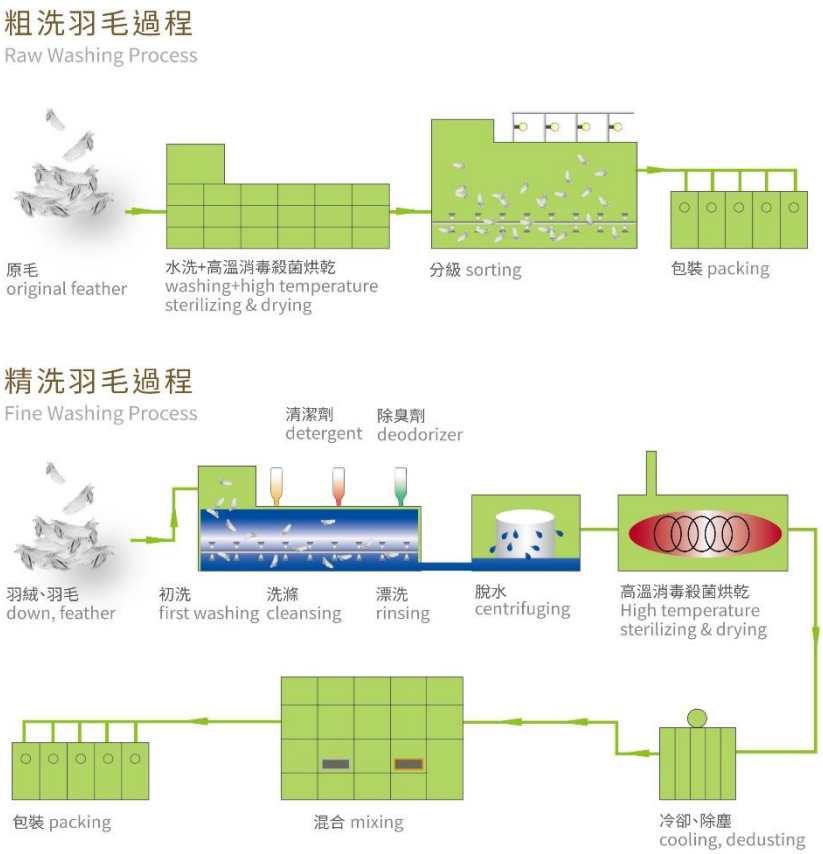

(a)

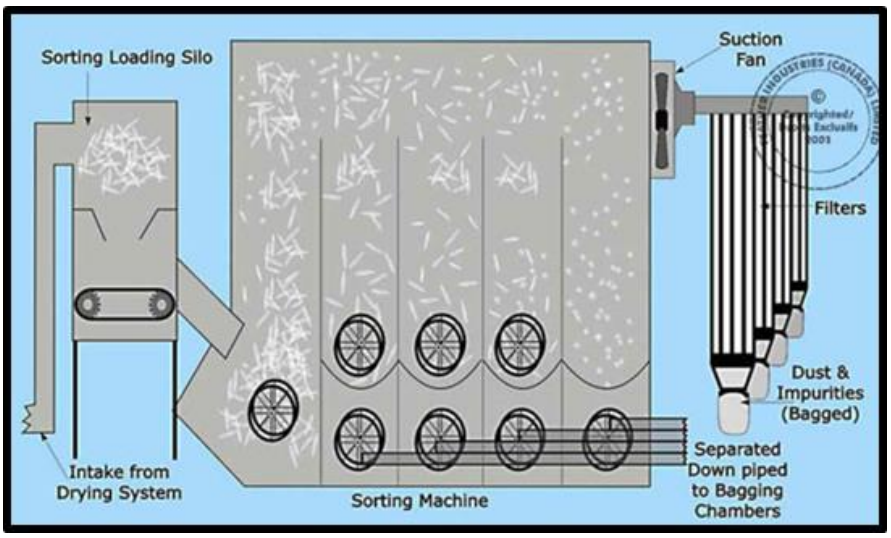

(b)

Figure 1.2: The mixed feather processing procedure includes (a) washing and (b) sorting in a series of vertical air channels [3, 4].

doi:10.6342/NTU202404295

This study uses dry feather mixture collected in the middle sorting bins from a commissioned supplier as the research samples. This batch of feathers faces two bottlenecks when we refine the sorting in air [5]. Firstly, this batch consists of feathers with larger sizes and longer fibers, as shown in Figure 1.3 (a), which tend to tangle into clusters of 4 to 15 centimeter-long, as shown in Figure 1.3 (b). The problem tends to recur and severely degrade the sorting results. Secondly, the conventional sorting process is time-consuming. Hence, a different sorting strategy is desired and attempted in this work.

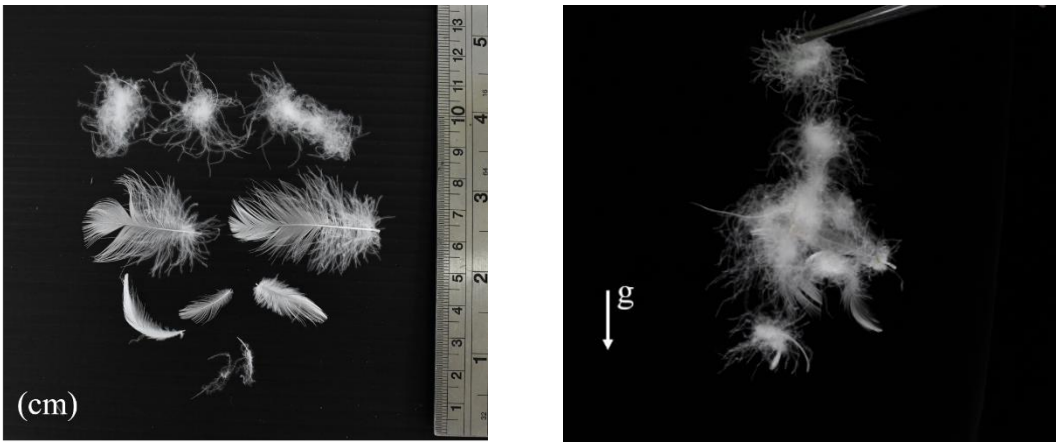

(a) (b)

Figure 1.3: (a) Feather samples used in this study.
(b) Clusters of tangled feathers, lifted and suspended in the air.

doi:10.6342/NTU202404295

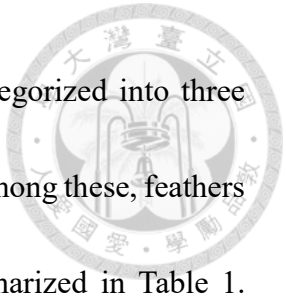

According to the supplier, the feather mixture samples are categorized into three types: feathers, downs, and others, as shown in Figure 1.4 (a) to (c). Among these, feathers and downs constitute nearly 95% of the sample's weight, as summarized in Table 1. Therefore, after further analyzing the differences in the appearance between these two [1, 6], we observe the following. The feathers to be sorted out in Figure 1.4 (a) have a structure characterized by a hollow root (known as the calamus) extending into a rigid rachis. From the root to the middle section of the rachis, there are soft and fluffy barbs extending outward, forming a three-dimensional structure. The middle to the end section of the rachis extends into longer and more rigid barbs in a flatter structure. In contrast, the downs to be collected in Figure 1.4 (b) have a structure consisting of a fluffy and more spherical arrangement of long fibers, with the filling density decreasing from the center to the rim. The rest ("others") includes fibers and impurities as shown in Figure 1.4 (c).

By manually picking out and examining the sample feathers, we observed differences in the appearance of feathers with a length of less than 4 cm and a width of less than 2 cm as compared in Figure 1.5 (a) and (b). Therefore, we further classified the feathers into big and small categories based on these dimension thresholds. Sorting for the small feathers and downs has been proposed by our group [5]. Thus, this research aims to address the separation of big feathers and downs. the maximum and minimum sizes of each type of feather are shown i**n** Figure 1.5.

doi:10.6342/NTU202404295

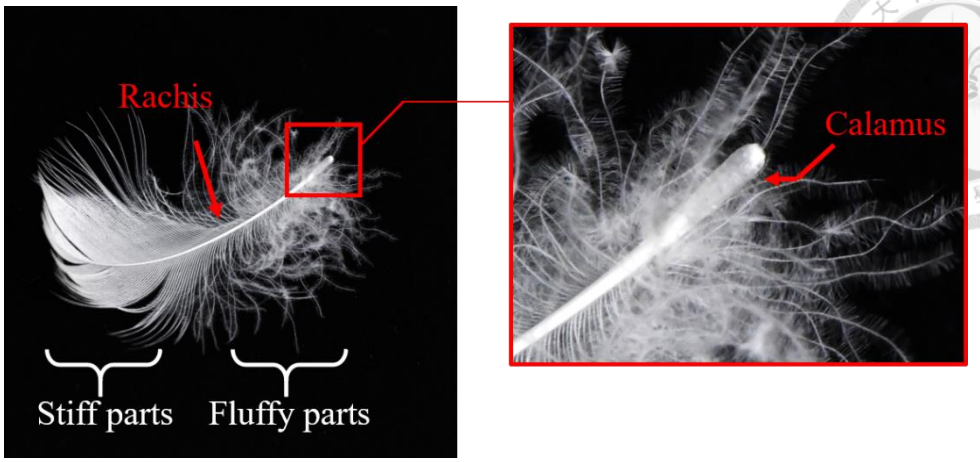

(a)

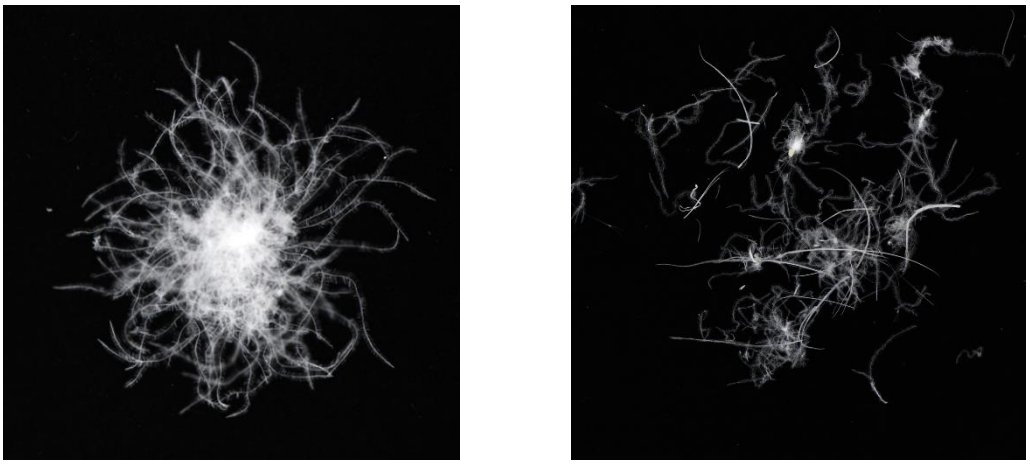

(b) (c)

Figure 1.4: The structural features of (a) feathers, (b) downs and (c) others in the current sample.

Table 1: The weight percentages of each type of feather in the current sample.

Downs	Feathers	Others
26.76%	68.29%	4.95%

doi:10.6342/NTU202404295

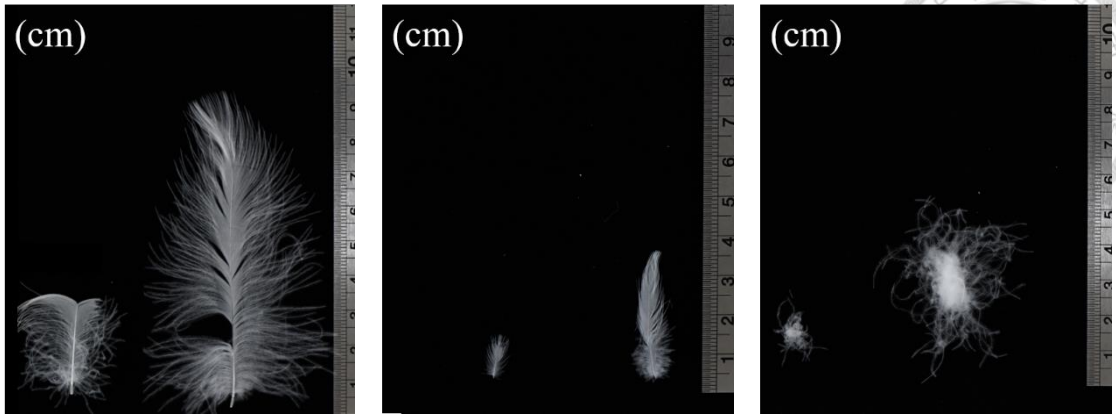

(a) (b) (c)

Figure 1.5: The size of (a) big feathers, (b) small feathers, and (c) downs in the sample.

Inspired by the series of washing steps in conventional feather sorting processes, we aim to separate big feathers and downs in aqueous environment. We first focus on identifying possible separation mechanisms and utilize then to design a sorting process. The proposed design achieves continuous immersion of samples, separation of big feathers, and collection of downs, which merge some of the washing and sorting procedures into a single streamlined process and may simplify the mixed feather processing process.

doi:10.6342/NTU202404295

Chapter 2 Working Fluid Formulation

This section describes how, in contrast to the conventional dry feather mixture sorting process, we discovered an effective wetting method for dry feather mixtures. Additionally, we report the differences between feathers and down feathers in their wetted state and how this finding is exploited to develop a separation method.

2.1 Wetting method for dry feather mixtures

To understand how dry big feathers and downs become wetted, we use tweezers to press both to the bottom of a 500 ml beaker filled with 25°C water, submerging them to a water depth of 10 cm. After being pressed to the bottom with tweezers for 24 hours, both types remained largely unwetted and remain floating after release. Such a surface unwetted condition was judged by the dazzling white portion, as shown in Figure 2.1. This indicated that the sample feathers used in this study possess water repellency [7, 8] and were difficult to be wetted in shallow water at room-temperature. Walker *et.al*. proposed a method to estimate the time required for a water solution to wet a test sample [9]. This method places the sample on the water surface and records the time it takes for the sample to completely disappear from the water surface. The immersion time shall indicate the wetting ability of an experimental solution.

doi:10.6342/NTU202404295

Following the wetting time estimating procedure, we randomly selected 10 big feathers and 10 downs with lengths in the range of 3 to 7 cm as our test samples for the static wetting time experiment. We chose this specific size as it is the most prevalent for both types in the sample. Each sample was placed individually on the surface of 25°C tap water and left for 24 hours. None of the samples showed any part of their volume immersed below the water surface. One set of test results is shown in Figure 2.2. Therefore, it is determined that the sample feathers used in this study exhibit extreme water repellency in tap water.

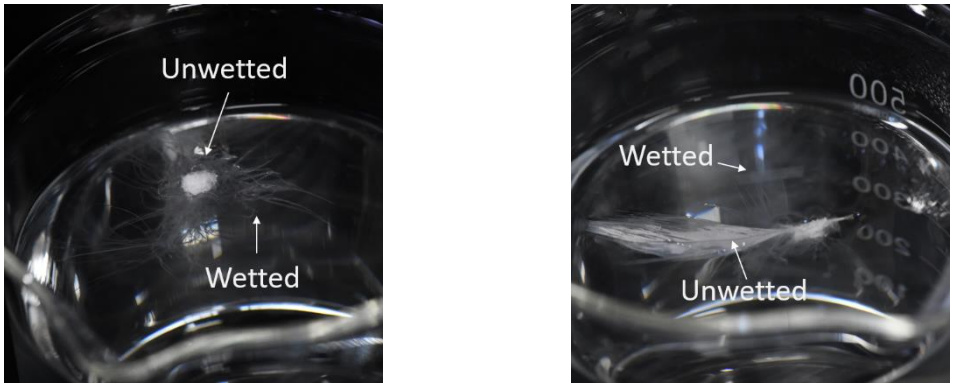

(a) (b)

Figure 2.1: (a) Down (b) Big feather after being submerged 10 cm under water and left for 24 hours. Both types of feathers were incompletely wetted and floated to the surface.

(a) (b)

Figure 2.2: Side view of (a) down and (b) big feather after the wetting time test.

doi:10.6342/NTU202404295

To drastically shorten feathers' wetting time, we try to reduce g the surface tension of the liquid by dissolving a surfactant (SINO-JAPAN CHEMICAL CO., LTD., SINOPOL 1907HFB, Polyoxyalkylene Alkyl Ether) in 25°C tap water [10]. The test data provided by the surfactant supplier in **Figure 2.3** shows that the surface tension of the solution decreased as the weight percent of the surfactant ($wt\%_s$) was increased. The surface tension remained nearly a constant value of 30±1 dyne/cm when the concentration is increased above at greater than 0.015wt%.

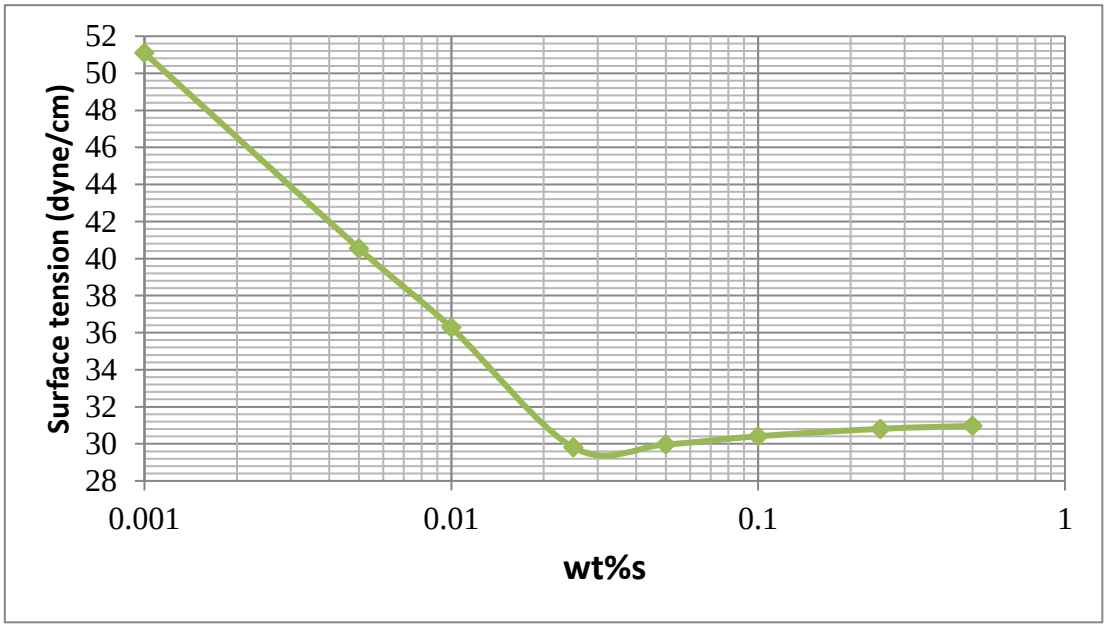

Figure 2.3: Plot of the surface tension of surfactant solution with respect to weight percent of the surfactant.

Hence, static feather wetting time measurement were first conducted using a solution with a surfactant concentration of $wt\%_s = 0.015$. The results shows that both the big feather and down were wetted and disappeared from the water surface in a time course of 1to 20 minutes, as shown in Figure 2.4.

doi:10.6342/NTU202404295

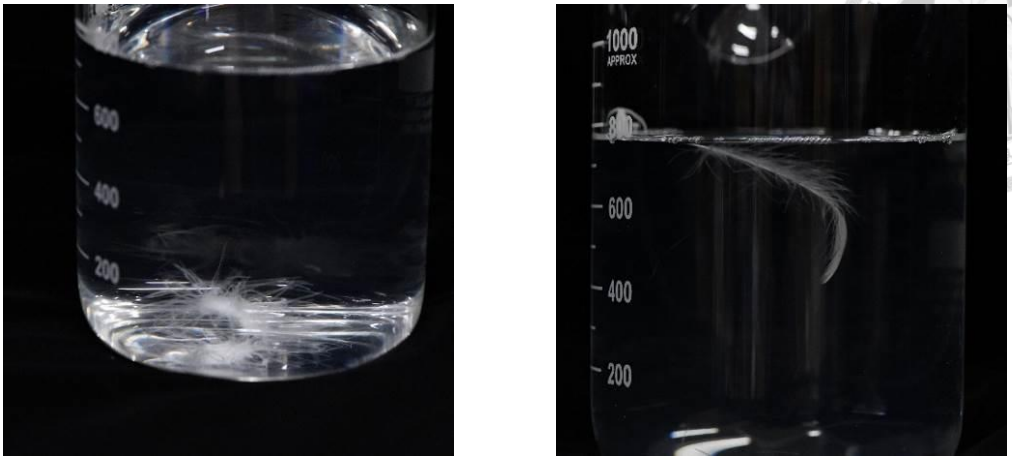

(a) (b)

Figure 2.4: (a) Down and (b) big feather disappear from the water surface after being completely wetted.

To further accelerate the wetting process, we considered the contact between the feather surfaces and the liquid by stirring the surfactant solution could. We used a stirring rod to stir, at 2rps, a 1000 g surfactant solution of $wt\%_s = 0.015$ in a 1000 ml standard beaker with big feathers and downs floating on the surface for 1 minute. We found that this dynamic wetting method significantly reduced the wetting time, even though some portions of the feathers still remain incompletely wetted, as shown in Figure 2.5. Subsequently, we continued stirring the solution at the same rate, stopping every minute to inspect the wetting status of the feathers. We found that after 2 to 6 repetitions of such a process, both big feathers and downs gradually became completely wetted. Through observation, we found that downs become incompletely wetted compared more easily than big feathers. Additionally, this incomplete wetting phenomenon occurs more frequently as the density of the barbs at the center of the down feathers becomes denser,

doi:10.6342/NTU202404295

as shown in **Figure 2.6**.

(a) (b)

Figure 2.5: Bright white, incompletely wetted areas appeared in (a) down and (b) feather after the initial 1-minute of stirring.

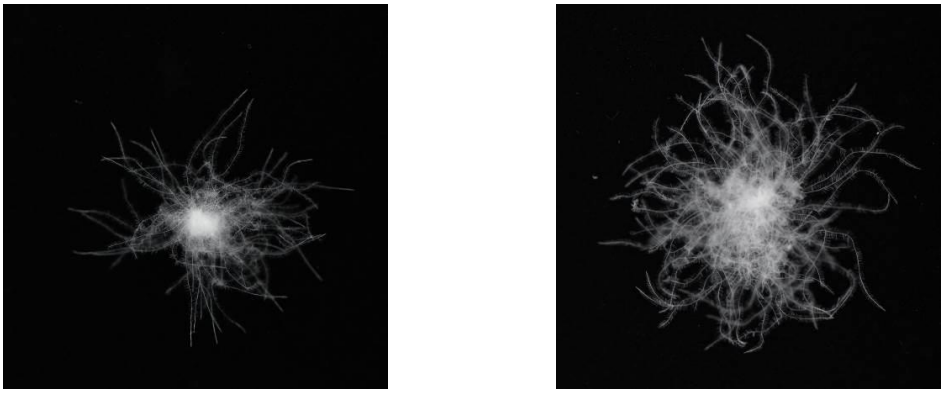

(a) (b)

Figure 2.6: The appearance of down with (a) denser (b) less dense center.

To further shorten the dynamic wetting time while ensuring both big feathers and downs were completely wetted, we tried to increase the surfactant concentration. It was found that, although the surface tension of the surfactant solution remained nearly constant above a critical surfactant concentration of 0.015 $wt\%_s$, there were signs of enhanced wetting for both big feathers and downs under the same operating time. Therefore, four surfactant solutions with different surfactant concentrations, including

doi:10.6342/NTU202404295

0.05 wt%$_s$, 0.15 wt%$_s$, 0.20 wt%$_s$, and 0.30 wt%$_s$, were prepared in four 1000 ml standard beakers to measure the effect of surfactant concentration on dynamic wetting performance. For each surfactant solution, 10 dry downs were randomly selected as test samples and placed on the surface of the surfactant solution. We only tested downs because previous observations revealed that the phenomenon of incomplete wetting occurred more frequently in downs compared to big feathers. A hand-held stirring rod was used to stir the solution clockwise at approximately 2 rps for 10 seconds, followed by counterclockwise stirring for 3 revolutions at the same speed to accelerate the cessation of the flow field, and then stirring was stopped. Observations were made within 1 minute to check if any downs floated to the surface due to incomplete wetting. The above procedure constitutes one operation. We continuously performed such an operation until all downs became completely wetted, and recorded the total number of operations.

Table 2 records the results of the testing times and the trend is shown in **Figure 2.7**, indicating that increasing the surfactant weight concentration does reduce the time to completely wet the downs by dynamic wetting method. Additionally, extending the dynamic wetting time allowed downs that were initially incompletely wetted to gradually become fully wetted. Furthermore, except for wt%$_s$ = 0.3, other experimental sets required more than one operation and showed less consistent wetting effects. Therefore, wt%$_s$ = 0.3 is identified as the most suitable surfactant concentration for this experiment.

doi:10.6342/NTU202404295

Table 2: The number of operations required to completely wet all downs in surfactant solution with different surfactant concentrations.

wt%s	Test 1	Test 2	Test 3	Average	STD
	Number of operations				
0.05	4	2	2	2.7	0.9
0.15	4	2	1	2.3	1.2
0.25	3	2	1	2.0	0.8
0.3	1	1	1	1.0	0.0

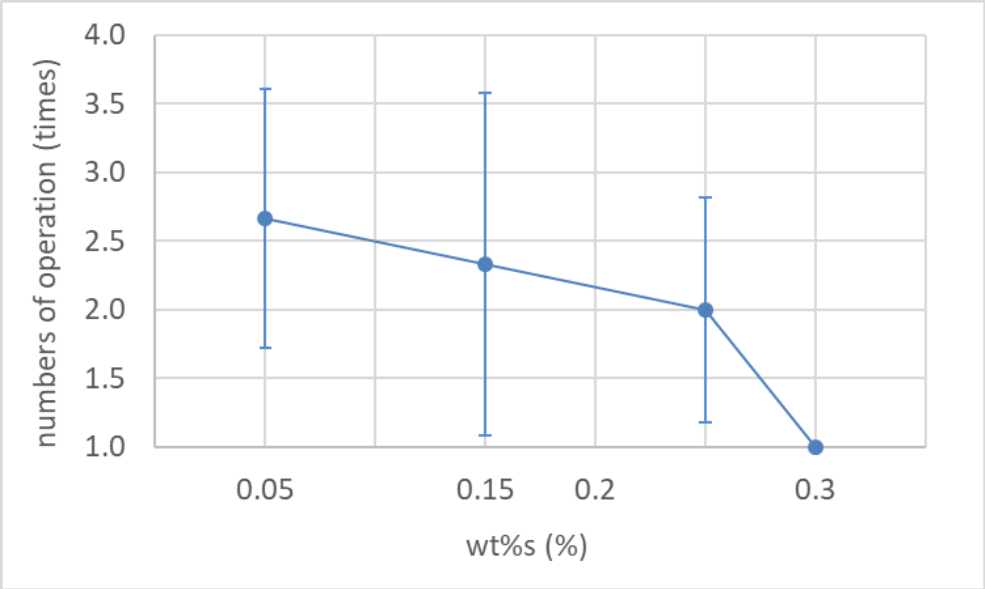

Figure 2.7: The number of operations required to completely wet all downs in surfactant solution with different surfactant concentrations.

Other than wetting feathers, we discovered an important factor affecting the dynamics of big feathers in the wetting experiments. which may influence their post-wetting movement. Bubbles were trapped inside the hollow structure of the calamus of the big feathers even after the feather fibers were fully wetted. As a result, big feathers

doi:10.6342/NTU202404295

had a higher tendency to float compared to fully wetted downs in a stationary liquid, as shown in Figure 2.4.

Nonetheless, this also inspired us to exploit the bubble-enhanced buoyancy as an efficient mechanism for segregating big feathers from downs. We therefore attempted to increase the density of the surfactant solution in an effort to promote the buoyancy acting on the fully wetted big feathers.

2.2 Feathers segregation method with buoyancy

2.2.1 Solution density

By dissolving different amount of sodium chloride (Iodized High-Quality Salt, TAIYEN) in water, we prepared brine of varying densities. The aforementioned fixed surfactant concentration of 0.3wt%$_s$ was then adjusted to 0.3 g of surfactant per liter of brine, which was then mixed into the brine. This mixture will hereinafter be referred to as brine with surfactant. We confirm that big feathers and downs can still completely wetted in these brines with surfactant using the dynamic wetting method. The subsequent investigation focused on whether the two types of feathers showed consistently different floating tendencies in quiescent brine with surfactant, for which we call a quiescent buoyancy test.

The density of the brine for buoyancy test was estimated by material tables so that

doi:10.6342/NTU202404295

we can determine the required weight percentage of salt for achieving a designated density at 25°C [11]. A specific weight of salt was added to tap water at 24°C to 27°C according to the concentration of brine obtained from the material table, and fully dissolved to roughly achieve the desired brine density. The brine's density was then measured using a hydrometer (tfv338, Taifong) with a precision of 0.001 g/cm³ and fine-tuned by changing the ratio of water to salt until the desired density was achieved. Once the density was fixed, the required volume of the brine for each experiment was recalculated based on the density and the precise weight of brine measured by a scale of an of 0.01 g precision to minimize volumetric measurement errors. After achieving the desired solution density, 3 grams of pure surfactant were mixed per liter of brine and stirred until fully dissolved, completing the preparation of the brine with surfactant. All brines with surfactant in this study were prepared using this procedure and operated under the aforementioned temperature conditions.

We first used the brine with surfactant of 1.1 g/cm³ density for a comparison of buoyancy test with that using a surfactant solution of 1.0 g/cm³ density (without added salt). Static buoyancy tests were conducted on both big feathers and downs using these solutions. Following the same selection method and criteria as described in section 2.1, a total of 15 big feathers and another 15 downs with lengths between 3~7cm were randomly selected as the testing samples Each group was placed on the surface of a respective 2700

doi:10.6342/NTU202404295

ml experimental brine with surfactant of 1.1 g/cm³ density. After stirring the brine with surfactant for 1 minute, the stirring was stopped and the testing samples were left to settle for 5 minutes. To minimize the interaction effects between the samples during the initial settling phase, a stirring rod was used to gently separate them. The samples were then left to settle for another 5 minutes before we recorded the sample's floating status to finish the buoyancy test.

After completing the experiment with the 1.1 g/cm³ brine, all testing samples were removed and rinsed once with 3000 ml of tap water. The samples were then tested again using the same experimental procedure in a surfactant solution with a density of 1.0 g/cm³ to compare their floating tendency.

The proportion of big feathers that remained floating on the surface was 5 out of 15 in the 1.0 g/cm³ surfactant solution, while it increased to 12 out of 15 in the 1.1 g/cm³ brine with surfactant. Figure 2.8 (a) and (b) show how big feathers resided in the two solutions. In contrast, all downs sank completely in both solutions, as shown in Figure 2.8 (c) and (d). Therefore, it can be confirmed that increasing the solution density is an effective method for separating the two types of feathers in a quiescent solution.

doi:10.6342/NTU202404295

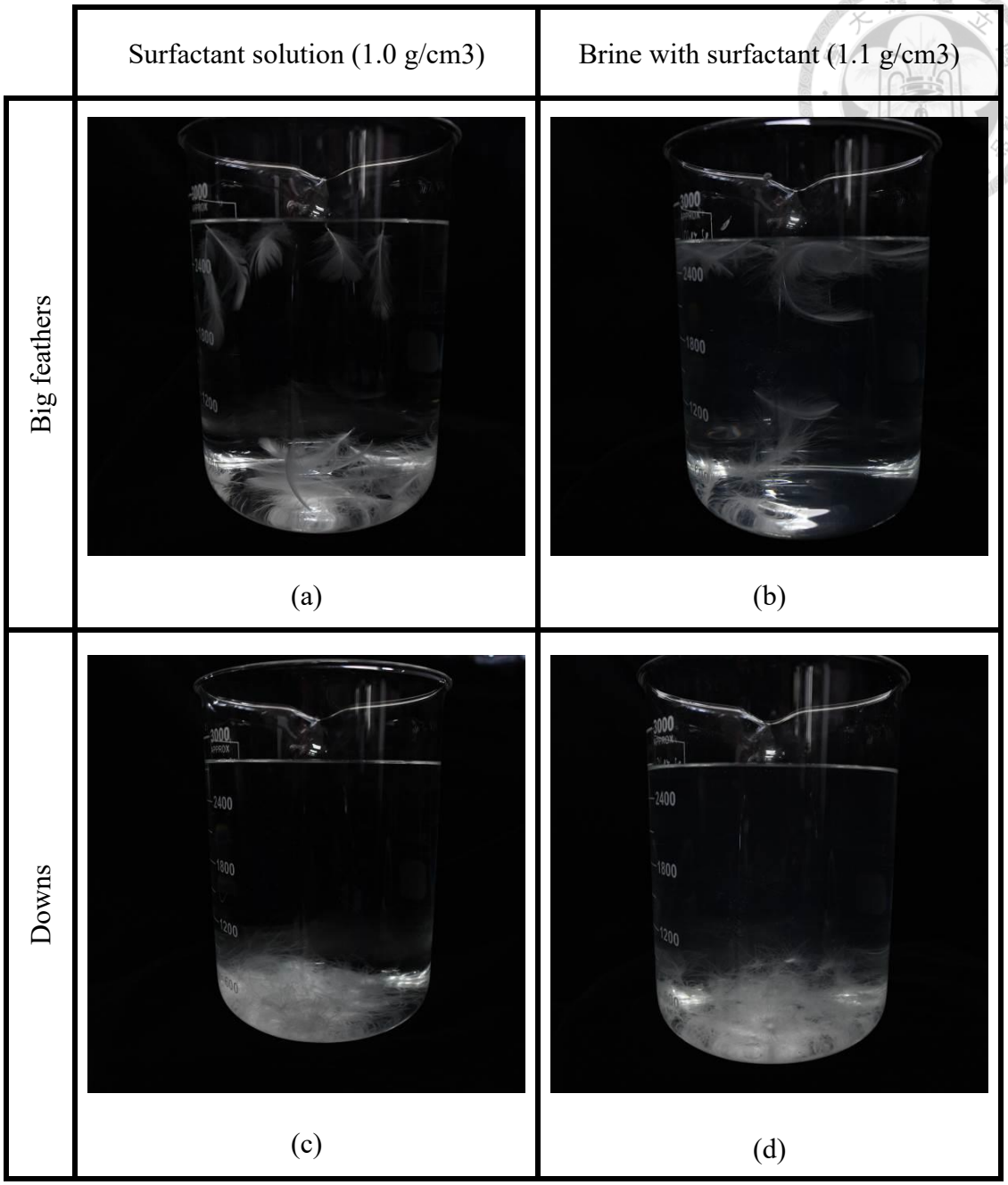

Figure 2.8: Results of quiescent buoyancy tests for two types of feathers in solutions of different densities: (a) Big feathers in 1.0 g/cm³ surfactant solution, (b) Big feathers in 1.1 g/cm³ brine with surfactant, (c) Downs in 1.0 g/cm³ surfactant solution, (d) Downs in 1.1 g/cm³ brine with surfactant.

It is worth noting that after feathers were soaked and left in the brine with surfactant for a period of time, many small and long-lasting bubbles appeared and adhered to both big feathers and downs. These bubbles increased the buoyancy of the previously sank

doi:10.6342/NTU202404295

downs, causing them to gradually rise to the surface, as shown in Figure 2.9. This refloating of downs would fail the buoyancy-driven segregation mechanism. One possible reason is that during the preparation of the brine with surfactant, the stirring action used to dissolve the salt may blend in a significant amount of air into the solution, which would dissolve again when liquid motion ceased.

Figure 2.9: Bubbles adhered to the big feathers and downs and caused them to float to the surface of the brine with surfactant after being left for an extended period.

Accordingly, after we prepared 500 ml brine with surfactant with a density of 1.1 g/cm^3, we placed it in a transparent and sealable glass bottle as the control group. Several randomly selected pieces of downs and feathers were placed on the water surface within

doi:10.6342/NTU202404295

5 minutes. After fully immersing them through stirring, the container was immediately sealed. The floating and sinking states of the control group after 10 minutes and 16 hours of sealing are shown in Figure 2.10 (a) and (b), for respectively. It was clearly observed that numerous small bubbles appeared, causing all the big feathers and downs in brine with surfactant to float on the surface after a long stand.

We then prepared another experimental group using the exact same solution preparation procedure with the addition of a degassing step. We let the solution stand in a sealed container for 30 minutes until numerous bubbles formed on the container wall. We manually scraped off these bubbles with a stirring rod before the dry feathers and downs were treated with the same immersion and resting procedures as used in the control group. The results of this experimental group after the same 10 minutes and 16 hours settling time are shown in **Figure 2.10** (c) and (d). Although a few small bubbles still appeared to cause one feather to float, the number and impact were significantly reduced. Thus, it can be confirmed that a degassing step during the preparation of the brine of surfactant was necessary to maintain the effectiveness of the subsequent buoyancy segregation method.

doi:10.6342/NTU202404295

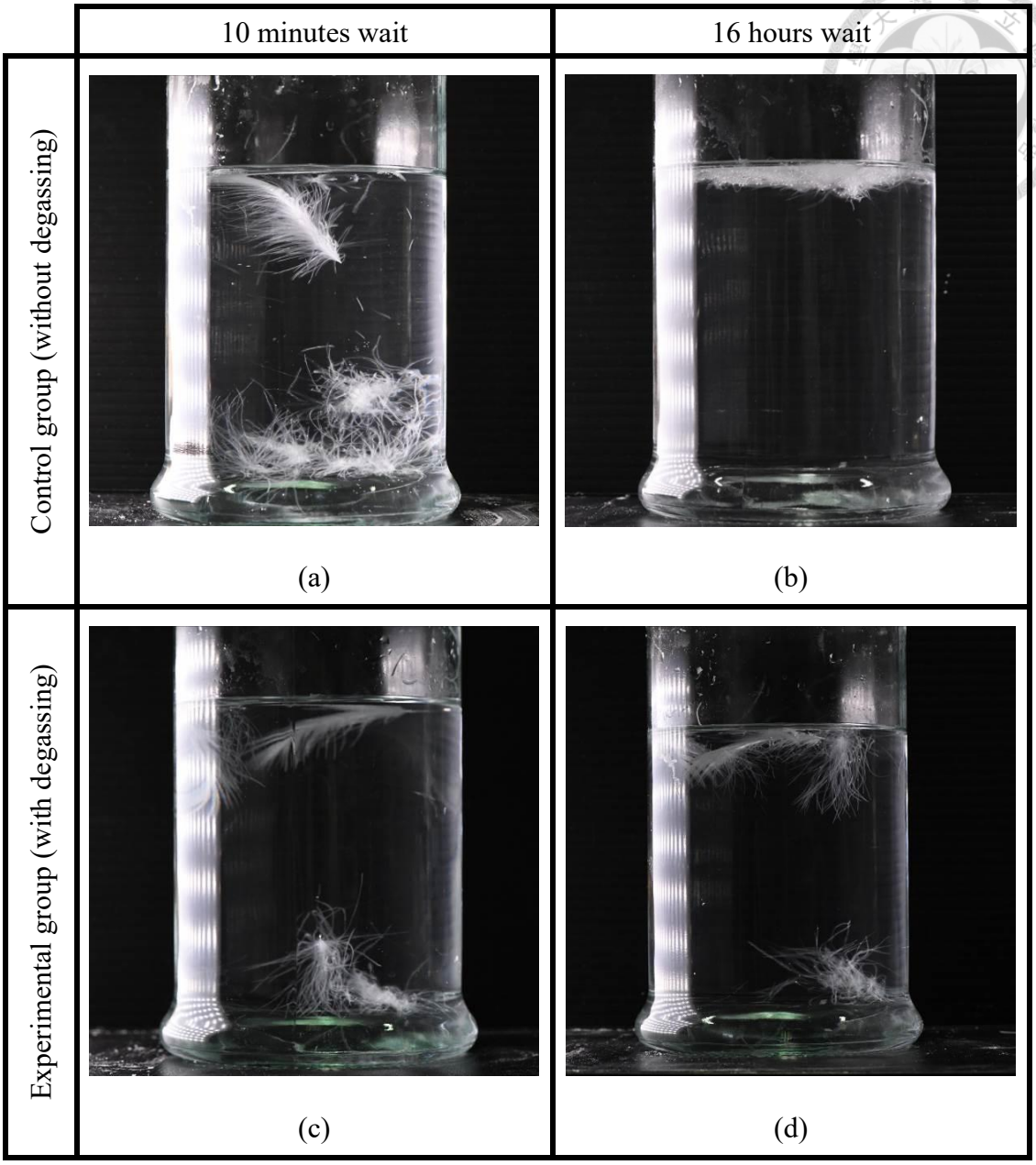

Figure 2.10: Test to show the effect of resolved bubbles that may cause the feathers and the downs to float together in the brine of surfactant of 1.1g/cm^3 density. The settling time for the control group is (a)10 minutes and (b)16 hours while the settling time for the experimental group is (c) 10 minutes and (d) 16 hours.

In summary, we improved the preparation process of brine with surfactant by sealing the container after following the original preparation steps to prevent evaporation-induced densification. We allowed the brine with surfactant to stand for 24 hours to let the

doi:10.6342/NTU202404295

dissolved air nucleate into bubbles, and used a stirring rod to slowly scrape away the bubbles adhering to the container wall for afterward, we maintained the sealed container and repeated the scraping process every hour until no more bubbles appeared.

2.2.2 Feather effective density

Besides the solution properties, we also needed information about the submerged feather mixtures. To analyze the density distribution of mixed feather samples after wetting, we first randomly selected 50 samples each of big feathers, small feathers, and downs as representative testing samples. These samples were subjected to density tests in a fully wetted state, for which a rinsing tank with 10 liters of surfactant solution at 0.3 wt%_s was prepared and used for the initial wetting. The density tests covered a range from 1.0 g/cm³ (without salt) to 1.19 g/cm³ (near-saturated salt concentration) in brine with surfactant, with increments of 0.01 g/cm³. For each density, two 1-liter containers of brine with surfactant of the same composition were prepared: one for pre-wetting and the other for testing.

Each type of feather sample was placed in the rinsing tank and stirred with a stirrer rod at approximately 1 rps in a clockwise direction for 1 minute. Afterward, the samples were allowed to stand for 5 minutes to inspect if there remains any bright white segment to ensure complete wetting. This process was repeated twice to ensure that all samples

doi:10.6342/NTU202404295

were fully wetted before the density tests that started from the solution of lowest density. The samples were first placed in the pre-wetting cup and stirred with a stirrer rod at the same rotational speed for 1 minute. This step aimed to prevent the wetted samples from carrying residual solution of different density to alter the test solution. After placing the samples in the testing cup, we stirred the mixture for 1 minute at the same speed and then let the mixture stand for 10 minutes until all motions were ceased. Whether the samples touched the liquid surface was used as an indicator to determine if their effective density was greater than or less than the density of the test solution. If the samples did not touch the liquid surface and remained submerged, we proceeded to the next test using a denser brine with surfactant, with the same rinsing-then-testing procedure.

We repeated the same testing procedure until all the samples were observed to float just beneath the free surface of the test solution to determine the feather's effective density. To present the experimental results, the number of feathers of a specific type N_i (where $i = D, BF, SF$) within each density range is divided by its initial total number $N_{0,i}$ to express the number ratio η

$$\eta = \frac{N_i}{N_{0,i}} \quad (2.1)$$

The number ratio η within each density range is represented as a percentage in Figure 2.11. The results showed that increasing the density of brine with surfactant can make a higher proportion of feather samples float while ensure all the down samples remained

doi:10.6342/NTU202404295

submerged. With a brine with surfactant density of 1.19 g/cm³, all the big feather samples can float while the down samples sank. Therefore, using saturated brine with surfactant in a static settling method should achieve the maximum static segregation effect of big feathers and downs.

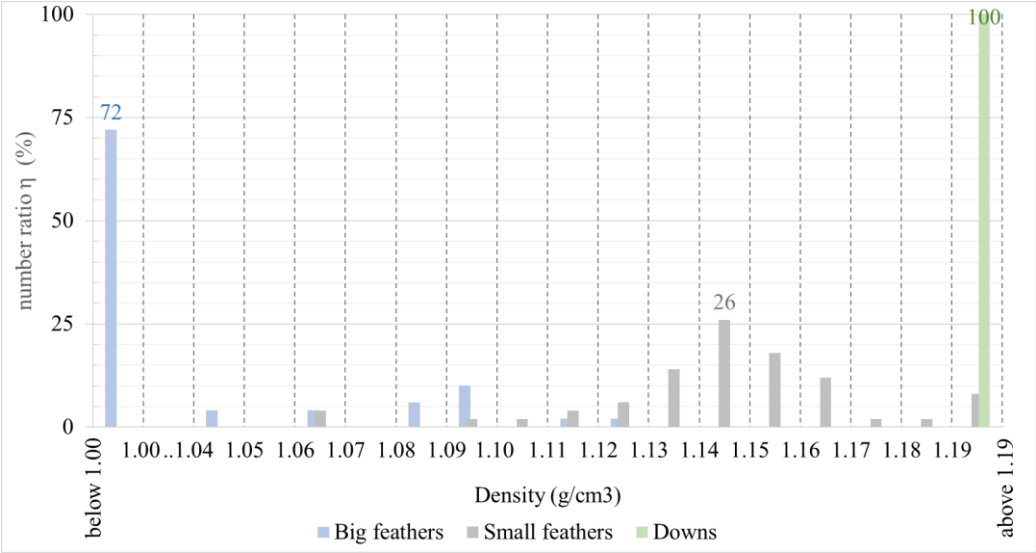

Figure 2.11: Density distribution ranges of various feather types in wetted state

2.2.3 Temperature effect

However, we also observed the change of transparency from clear to opaque as the density of brine with surfactant increased, the appearance of the solution changed from transparent to turbid due to the presence of surfactants, as shown in Figure 2.12, significantly degrading the observation of feather movement.

We suspect that the color change is related to the temperature effect on the surfactant so that additional experiment was conducted to correlate brine with surfactant's transparency to its density and temperature. We found that brine with surfactant of greater

doi:10.6342/NTU202404295

density needs to be at a lower temperature to remain transparent. The current brine with surfactant of 1.1 g/cm³ density began to turn opaque at approximately 28.5°C when we slowly heated it from 25°C using a water bath, as shown in **Figure 2.12**(a) and (b), which was slightly higher than the room temperature with indoor air conditioning during our experiments. Hence, we raised the density by adding salt to 1.15 g/cm³, which lower the critical temperature for turning opaque to approximately 25°C. Hence, we raised the density by adding salt to 1.15 g/cm³, which caused the solution to remain opaque at 25°C, as shown in Figure 2.12 (c) and (d). Therefore, we aimed to reduce the brine with surfactant's density from 1.19 g/cm³ to the level that can still achieve buoyancy segregation effects on the feathers while avoiding the need for additional cooling equipment to simplify the experimental setup.

(a)

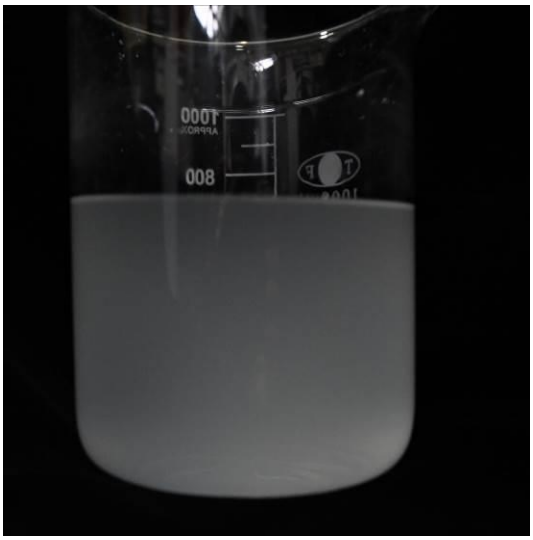

(b)

doi:10.6342/NTU202404295

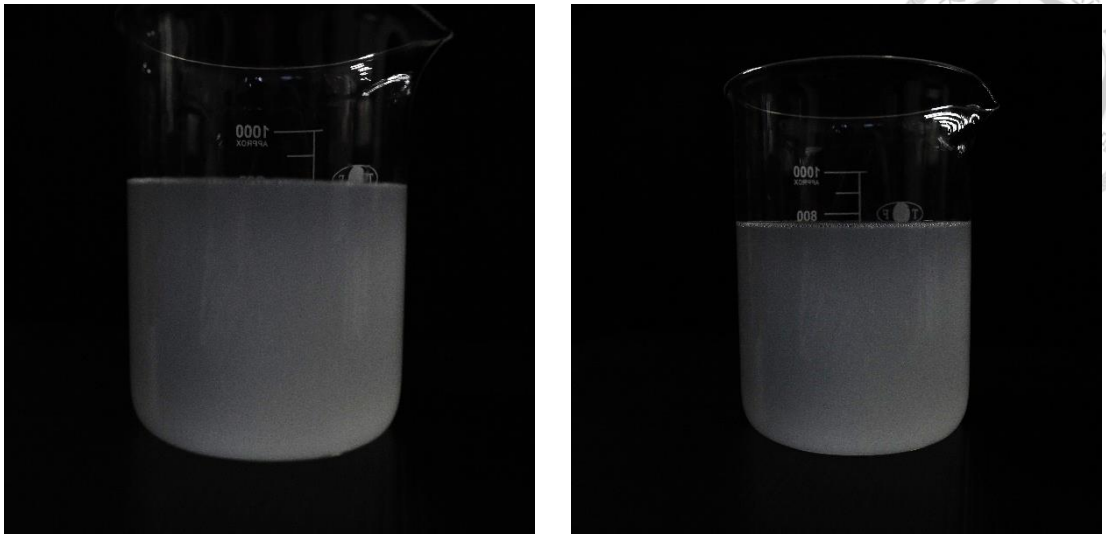

(c) (d)

Figure 2.12: The appearance of brine with surfactant with a density of 1.1 g/cm³ was as follows:
(a) transparent at 25°C； (b) turbid at 28.5°C.

Considering the effectiveness of segregation, observational feasibility, and reduction of experimental complexity, the final working liquid formulation used in this study was brine with surfactant with a density of 1.1±0.002 g/cm³ and a weight ratio of solution to surfactant of 1000:3. This choice was made under the condition of maintaining the experimental environment at 25 ± 2°C with indoor air conditioning. Furthermore, based on the previous test results, we expected the static buoyancy segregation mechanism to be capable of separating 95% of the big feathers from the mixed feather samples.

doi:10.6342/NTU202404295

Chapter 3 Experiment Apparatus

Having discussed the methods for wetting dry feather mixtures and buoyancy segregation mechanism in Chapter 2, this chapter will describe the immersion flow field experimental apparatus we designed to achieve a continuous feather sorting process. This apparatus used the brine described in the Chapter 2 as the working fluid, combined with detailed flow field design, to aim for the separation of 90% of big feathers from the dry feather mixtures. Simultaneously, the setup would collect the remaining feather mixtures after the operation. To help with future optimization and manufacturing, we also analyzed the percentage of down feathers relative to their initial state after the operation by the apparatus.

This chapter contains four sections. The first section introduces the comprehensive framework of the apparatus, including the specifications of each component and their respective application. The second part presents full details regarding the operational flow field and the validation of segregation mechanism operating within the flow field. The third section provides detailed information on the primary adjustable parameters and procedures for experiments used for the primary experiment. The fourth section analyzes the primary experimental results.

doi:10.6342/NTU202404295

3.1 Framework of the Apparatus

The overall experimental setup of this study is a liquid circulation system, as shown in Figure 3.1. The pump located at the lower left corner as shown in Figure 3.1 (1) was the beginning of the flow. Following the direction indicated by the blue arrows in the diagram, the experimental fluid flows from the upstream to the downstream, passing sequentially through the fluid inlet piping system (Figure 3.1 (2)), the experimental water tank (Figure 3.1 (3)), and the fluid outlet piping system (Figure 3.1 (4)), before returning to the pump, thus completing the circulation

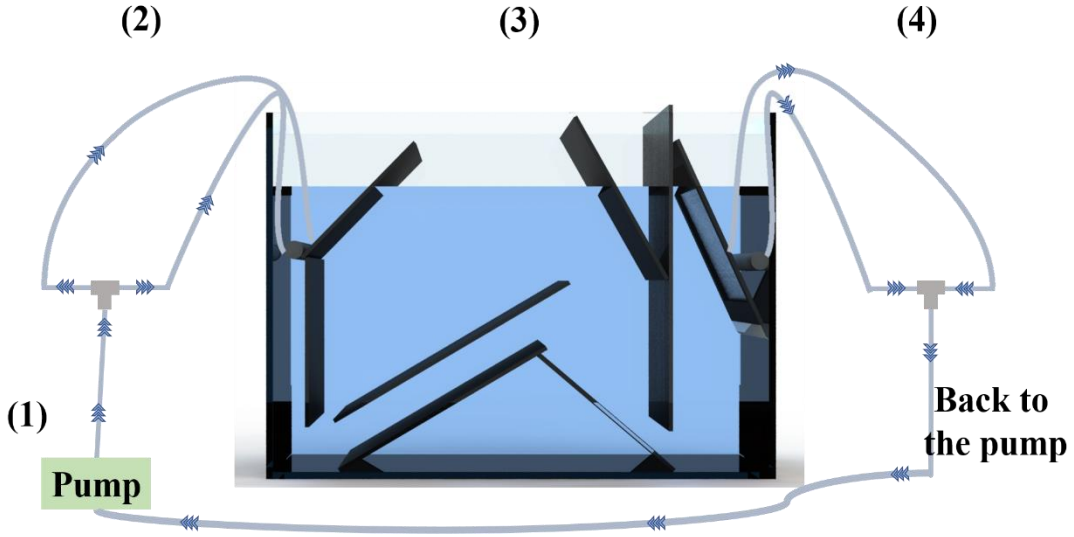

Figure 3.1: Schematic diagram of the experimental apparatus.

The working fluid used is the brine with surfactant prepared according to the formulation introduced at the end of Chapter 2 A flow channel was created in the water tank to generate a controllable flow field, with the goal of dynamic feather mixtures

doi:10.6342/NTU202404295

wetting, transport, separation, and collection of big feathers and downs. The flow input and output pipe systems define the upstream and downstream of the tank. The origin of the Cartesian coordinate system is defined at the midpoint of the upstream bottom edge of the water tank, as shown in Figure 3.2. The X-axis extends from the upstream to the downstream, and the Y-axis extends from the bottom of the tank to the water surface. In this paper, the coordinate system is represented by uppercase XYZ, with lowercase xyz indicating directions along these axes.

To ensure that the flow fields in the experimental tank were not overly complex and difficult to analyze, the equipment setup, except for the pump and external pipe systems, is designed to be symmetrical. The symmetrical plane is defined as the X-Y plane, as shown by the blue cross-section in Figure 3.2. During the flow field experiments, a camera was positioned parallel to the Z-axis to record the flow field Additionally, a flat-panel photography light is placed above the water surface, parallel to the Y-axis, to provide illumination, as depicted in Figure 3.2. The following sections describe the specifications and configuration of each component in the apparatus.

doi:10.6342/NTU202404295

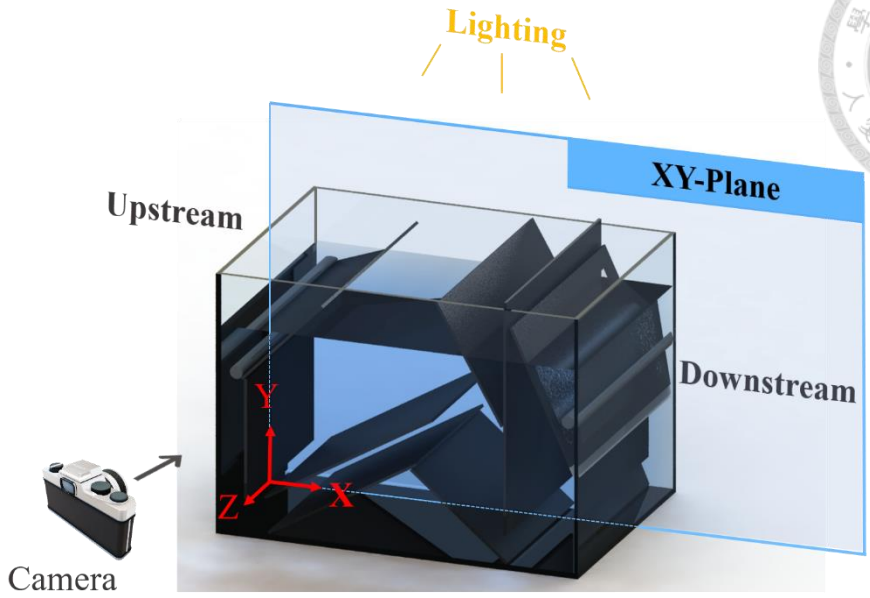

Figure 3.2: Schematic diagram of the coordinate system, symmetry plane of internal components, and experimental image recording methods.

3.1.1 Pump

As the upstream fluid driver of this experimental setup, we used the "Marine DC Pump 3000" as the fluid driver, which included the pump body and controller, as shown in Figure 3.3. The inlet and outlet diameters of the pump were both 1.6 cm, and it could be connected using a 2.2 cm inner diameter hose fitted over the outer circumference., as shown by the green hose in Figure 3.3(a). The pump had a rated flow rate of 3000 L/H and had 100 adjustable power output levels.

doi:10.6342/NTU202404295

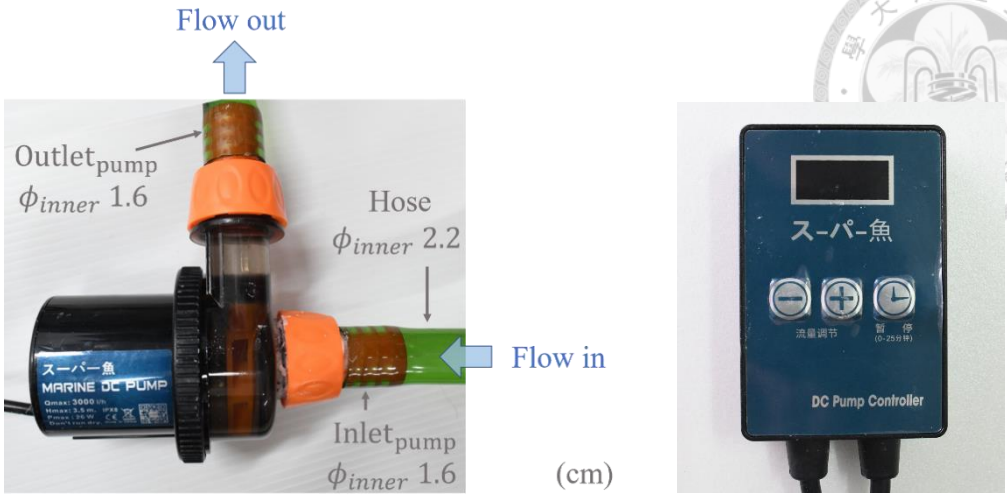

(a) (b)

Figure 3.3: (a) pump and (b) flow rate controller of inlet piping system.

The inlet piping system was designed to channel the fluid from the pump into the tank and generated jets flow to drive the internal flow field, as shown in Figure 3.4. The piping system, designed to match the pump's outlet diameter, used a hose with an internal diameter of 2.2 cm for connection, as shown in Figure 3.4 (a). This hose extended 330 cm and connected to a T-type equal tee, as shown in Figure 3.3(a-I), Figure 3.4 (b), which then branched into two equivalent 60 cm hoses, as shown in Figure 3.3(a-II) (c). Each hose connected with a 90-degree L-elbow at the end, as shown in Figure 3.4(d). Since both types of connectors had an internal diameter of 2.2 cm and an external diameter of 2.9 cm, they could not directly connect to the 2.2 cm internal diameter hose. In order to bridge this gap, we used short PVC pipes with a 16 cm internal diameter, a 22 cm external diameter, and a length of approximately 6±1 cm, as shown in Figure 3.4(b), (e).

doi:10.6342/NTU202404295

We connected two 90-degree L-shaped elbows to each ends of a long PVC pipe with 60 equally spaced circular holes along its length, which we referred to as the inlet pipe. The fluid flowed out of this pipe in a sequential jet stream. The diameter of the circular holes was 0.3 cm, with a center-to-center spacing of 0.5 cm. The whole length, including L-shaped elbows and the pipe, was 42 cm, as shown in Figure 3.4(f). To create these holes on the inlet pipe, a laser cutter first marked the circular holes in the inlet pipe's wall, creating positioning holes with a diameter of 0.1 cm. We used a fixed drilling machine with a 0.3-cm drill bit to drill from top to bottom through the vertical alignment of the positioning holes. Every five holes in the process, we checked the distance between the vise jaws and the positioning holes to ensure equal spacing, preventing deviations and ensuring the drill angle remained vertical. This mechanical drilling method was used to prevent the occurrence of plastic melting caused by laser cutting, which could result in unevenly sized holes.

Finally, the inlet pipe was positioned symmetrically along the X-Y plane within the experimental water tank, 10 cm below the fluid surface, and at a 45-degree counterclockwise angle relative to the horizontal X-axis. The holes in the pipe directed a continuous jets flow towards the water surface to drive the surface and internal flow fields within the tank, as shown in Figure 3.4(a-III). This component, with its symmetrical setup of the pipeline and discharge pipe, ensured that the fluid exited the discharge pipe as

doi:10.6342/NTU202404295

symmetrically as possible relative to the X-Y plane, closely quasi-2D flow field assumption. The symmetrical configuration of the pipeline and inlet pipe in this component ensured that the fluid exited the inlet pipe in an symmetrically with respect to the X-Y plane, thus closely approximating the assumption of a quasi-2D flow field.

It is worth noting that we observed a significant amount of foam entering the water tank along with the jet stream when the pump was first activated, which affected the experiment, as shown in Figure 3.5 (b). We speculated that the issue was due to the fact that the piping was not made as a single piece, which might allow air to enter and form foam due to the surfactants in the fluid. Therefore, before starting the formal experiments, the pump was first activated for about 10 minutes to allow any air within the piping to be fully expelled and the foam in the water tank to dissipate completely, as shown in Figure 3.5 (c) (d). The feather samples were added and tested only after this process was completed.

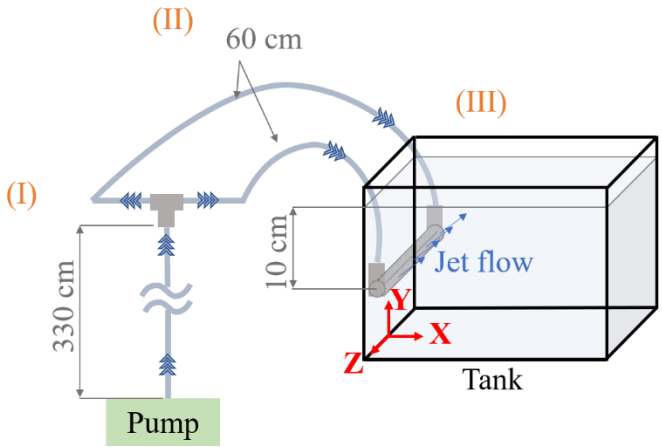

(a)

doi:10.6342/NTU202404295

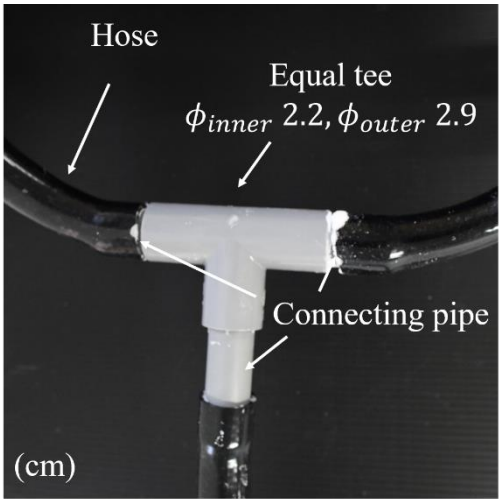

(b)

(c)

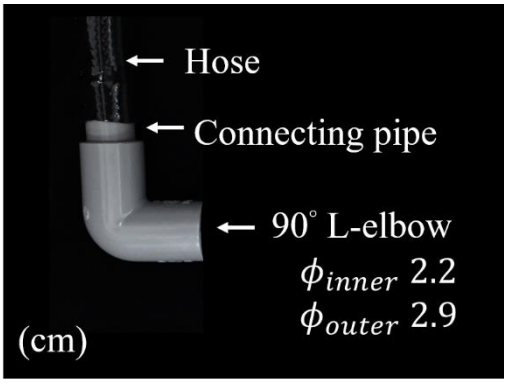

(d)

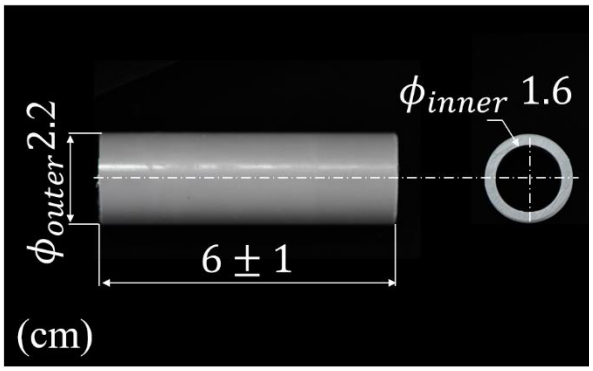

(e)

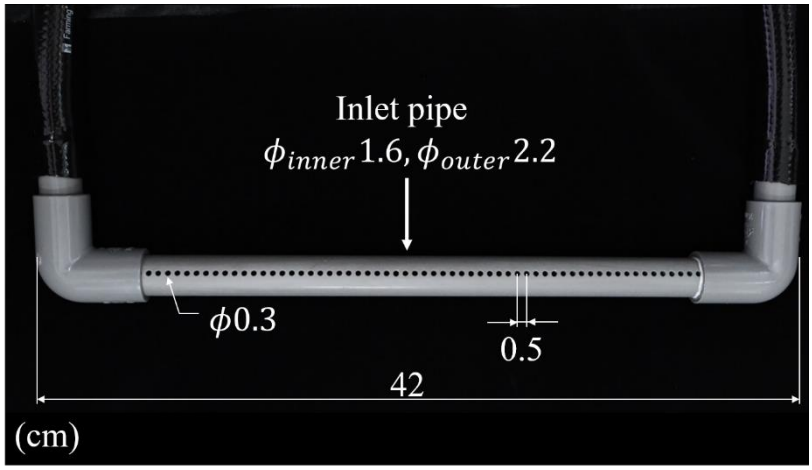

(f)

Figure 3.4: (a) Schematic diagram of inlet piping system; (b)T-type equal tee; (c) Flow direction after branching into two equivalent hoses; (d)90° L-elbow; (e)connecting pipe; (f)inlet pipe with $60 \times \phi 0.3\ equi-spaced\ holes$.

doi:10.6342/NTU202404295

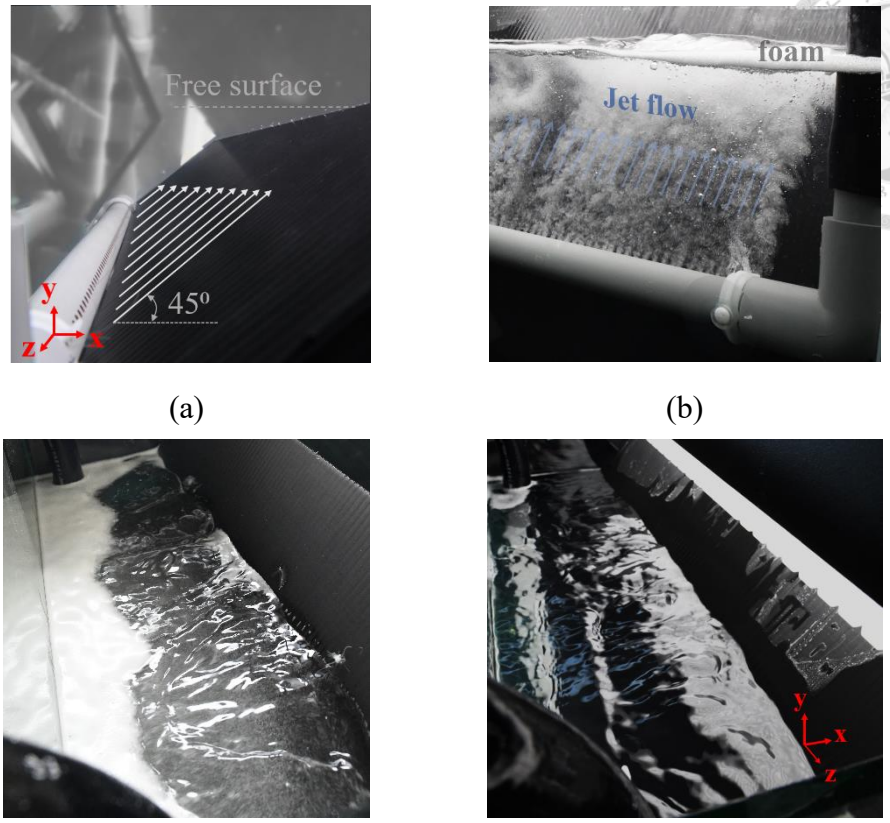

Figure 3.5: (a)Direction of jets flow；(b)jets flow with foam；
Surface foam situation after pump started: (c)10sec (d)10minutes.

3.1.2 Experimental tank and internal boundaries

As the working field for feather wetting, separation, and collection, this rectangular water tank is made from transparent glass with a thickness of 8 mm. The internal dimensions are 62 cm in the x-direction (length), 44 cm in the y-direction (height), and 44 cm in the z-direction (depth). Throughout the experimental process of this study, the solution height inside the tank is maintained at 35±0.1 cm. The fluid entered the tank in the form of an immersed liquid flow through the inlet pipe, as shown in Figure 3.6 (I), then passed through the flow channel we designed, as shown in Figure 3.6 (II), the feather

doi:10.6342/NTU202404295

collection strainer, as shown in Figure 3.6 (III), and ultimately exited the tank via the outlet pipe, as shown in Figure 3.6 (IV).

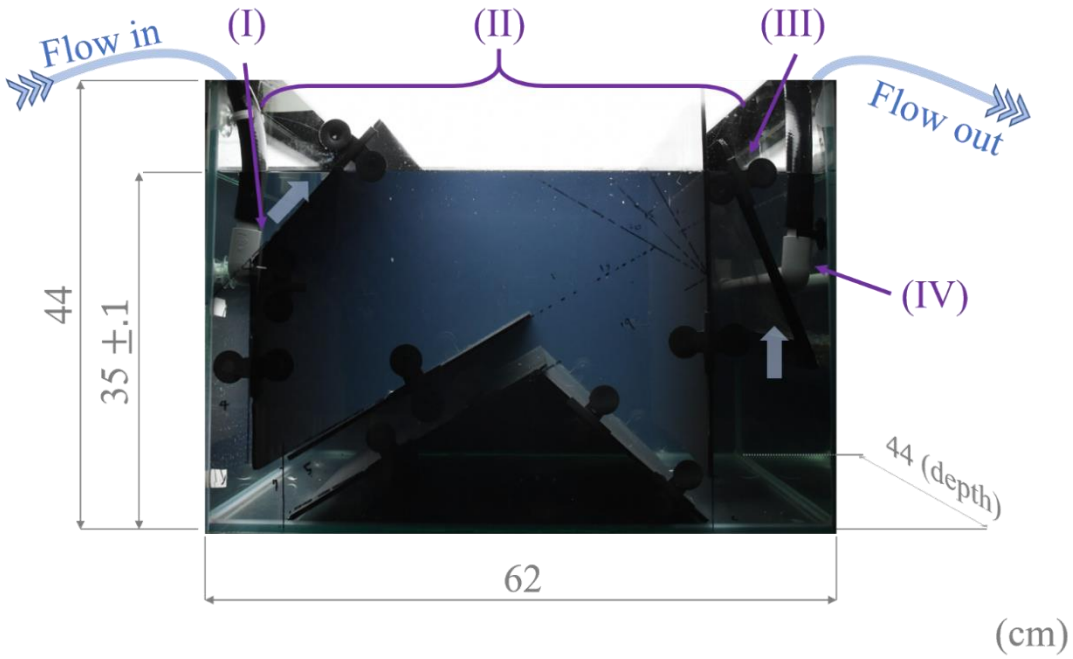

Figure 3.6: Dimensions of the tank and internal component layout diagram.

In order to easily adjusted the flow field for extensive trial-and-error design and observation of feather movement, all flow channel boundaries in the experimental setup needed to be adjustable and cost-effective. Therefore, we used 0.5 cm thick black polypropylene (PP) corrugated board to build the flow field boundaries, as shown in Figure 3.7 (a). This material was chosen due to its affordability, availability, and ease of cutting.Nevertheless, the board's hollow core structure could trap air, increasing buoyancy, and its large surface area within the flow field made it susceptible to displacement due to fluid pressure changes. Therefore, a fixing method that allowed for

doi:10.6342/NTU202404295

position adjustments while still providing sufficient strength to resist displacement under fluid pressure is required. To address this issue, we used aquarium isolation clips to hold the PP boards and suction cups to attach them to the glass tank walls, as shown in Figure 3.7 (b). It is worth noting that the shape of these clips created unavoidable gaps between the PP corrugated board and the glass tank. After evaluation, all gaps were found to be less than 0.05 cm, as shown in Figure 3.7(b) (c). Therefore, we assumed that their impact on the flow field were negligible. This method provided significant flexibility in adjusting the geometric configuration of the flow channels while maintaining a reasonable level of dimensional accuracy and acceptable seal quality.

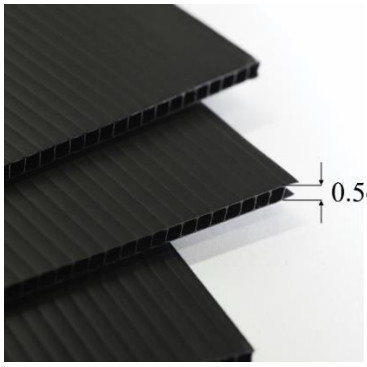

(a)

doi:10.6342/NTU202404295

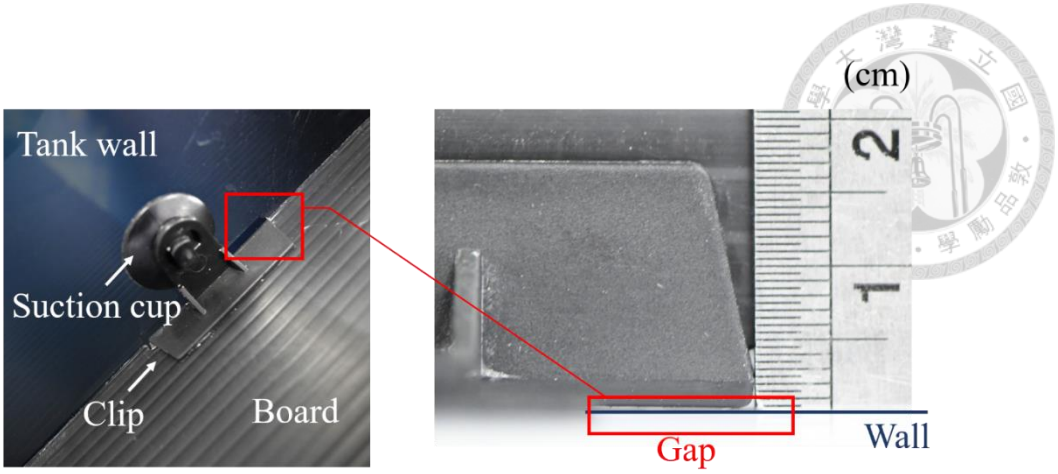

(b) (c)

Figure 3.7: (a) polypropylene (PP) corrugated board.

3.1.3 Outlet piping system

The outlet piping system was designed to channel the fluid from the tank back to the pump, completing a circulation. Conceptually, this system was the inverse of the inlet piping system, with variations in hose lengths, positions, and the outlet pipe configuration according to the spatial arrangement and the pump's relative position. The outlet pipe, which was identical in size and hole count to the upstream inlet pipe, was positioned 12 cm below the liquid surface in the tank, with its holes facing directly towards the bottom of the tank. Fluid was sucked into this outlet pipe and then flowed from the two sides of the outlet pipe through 90-degree L-shaped elbows and entered two 30 cm long, equally sized hoses. The ends of the two hoses converged through a T-type equal tee and were then connected via a 220 cm long hose to the pump, completing the cycle, as shown in Figure 3.8.

doi:10.6342/NTU202404295

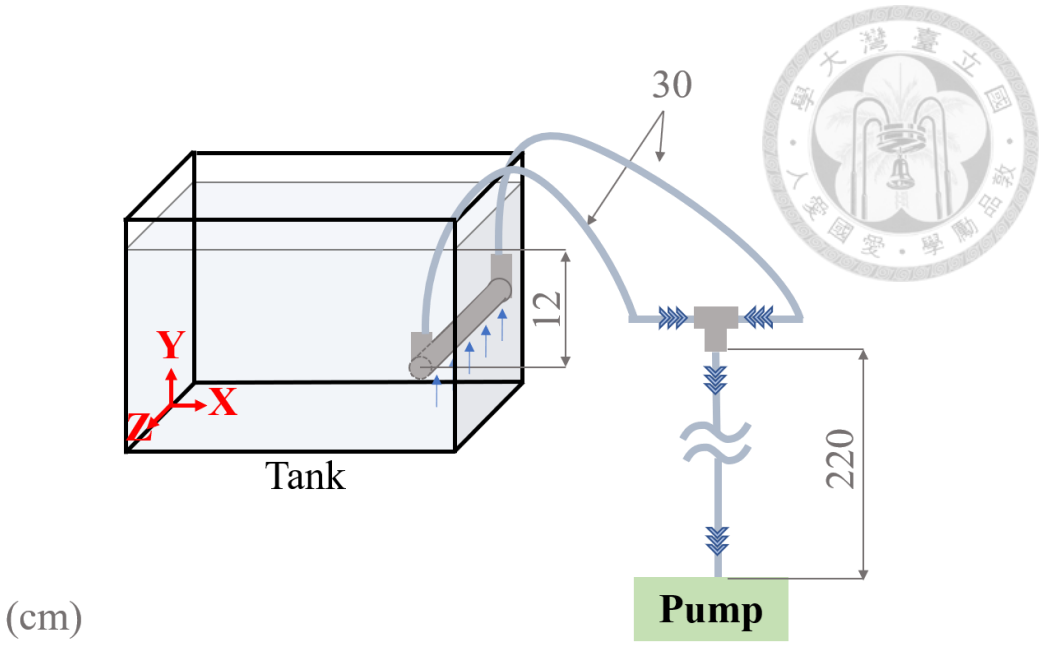

Figure 3.8: Schematic diagram of outlet piping system.

Additionally, we custom-made a strainer and placed it in front of the outlet pipe to collect the separated feather samples and prevent them from entering the outlet piping system and potentially damaging the pump. The strainer was made of the same PP corrugated board to create a rectangular frame with 1 cm in thickness and 3 cm in width. A 20-mesh stainless steel screen was fitted in the center, and the bottom was adhered with a 0.25 mm thick plastic sheet extending 2 cm outward using hot melt adhesive, as shown in Figure 3.9 (a). The strainer was fixed to the vertical wall of the water tank at a 25-degree angle relative to the outlet pipe using the same aquarium isolation clips, and its plastic sheet at the bottom was pressed against the water tank wall to enhance the seal, as shown in Figure 3.9 (b).

doi:10.6342/NTU202404295

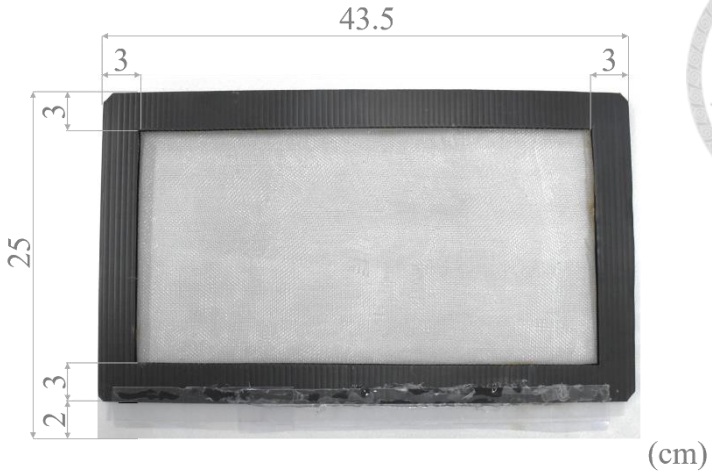

(a)

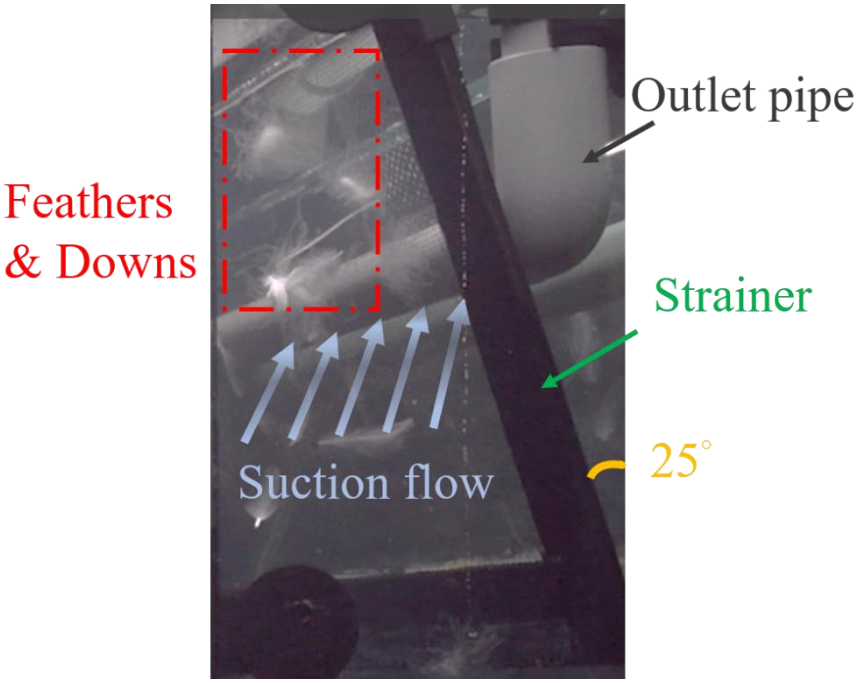

(b)

Figure 3.9: Figure 3.9: (a)strainer； (b) The strainer, which was positioned obliquely in front of the output pipe, collected feather products after the operation.

3.1.4 Actual flow rate measurement

After extensive trial and error, we found that a flow rate that was too low could not provide the necessary fluid forces for the feather samples to complete the expected

doi:10.6342/NTU202404295

movement path, On the other hand, a too high flow rate led to the predominance of fluid forces over buoyant forces, causing the desired separation mechanism to fail. Thus, it was determined that operating the pump at 70% power was a more widely applicable configuration for various flow field boundary setups during the testing. Consequently, this power level of pump was fixed for all following trials.

To measure the actual flow rate driven by this pump power setting, we fully assembled all components of the apparatus according to the method described in section 3.1, then took out the outlet pipe from the experimental tank and used it to direct the fluid into the measuring device. The measuring device consisted of a wide, shallow container with dimensions of 53 × 42 × 13 cm, placed on a high-capacity scale with a 10 kg load limit and 1g accuracy. The total mass of the fluid expelled from the outlet pipe was measured using this setup, while a smartphone recorded the scale readings at 120 FPS in slow motion. We calculated the time required to move 1 kg of fluid, which allowed us to estimate the actual flow rate. To ensure stable flow rate data, measurements taken during the first and last 5 seconds of pump operation were excluded. After five tests, the actual mass flow rate was estimated to be 0.398± 0.004 kg/s. Considering the fluid density of 1.10 kg/L at 25°C, the average flow rate was calculated to be 1302.55 ± 13.09 L/h, which is approximately 62% of the rated flow rate. Any variation in flow rate due to the permissible fluid density range of ± 0.002 kg/L would result in a change of less than

doi:10.6342/NTU202404295

±0.2%, which was considered negligible.

Based on the actual flow rate obtained from the measurement above, along with the dimensions and number of holes in the discharge pipe, and assuming negligible flow resistance within the discharge pipe and uniform jet intensity, the average flow velocity of a single jet was estimated to be 85.31 ± 0.86 cm/s. Assuming an average distribution of inlet flow along the Z-axis, the estimated two-dimensional average flow rate was 8.22 ± 0.08 cm^2/s.

3.1.5 Internal Flow Channels in the Tank

This section introduces the design and functions of the different flow channels at various locations within the experimental tank. Using a 1g dry feather mixed sample for each test, different geometric designs of flow channels were created inside the tank using PP boards and be tested under a fixed driving flow rate discussed in Section 0,. After extensive trial and error, the final flow channel configuration as a projection on the X-Y plane under the assumption of a nearly quasi-2D flow field is shown in Figure 3.10. Starting from the upstream inlet pipe, the fluid first flowed through the upstream entrain-disengaging zone, marked by the green dotted line (1) in Figure 3.10, near the water surface at the top left corner. It then passes through two transport channels, indicated by the purple dotted lines (2) and (3) in Figure 3.10. The fluid then entered the segregation

doi:10.6342/NTU202404295

zone, marked by the red dotted line (4) in Figure 3.10. Finally, , the orange dotted line (5) in Figure 3.10 depicts the product collection zone in the downstream area on the right. The functions and mechanisms of each of these zones are described as follows:

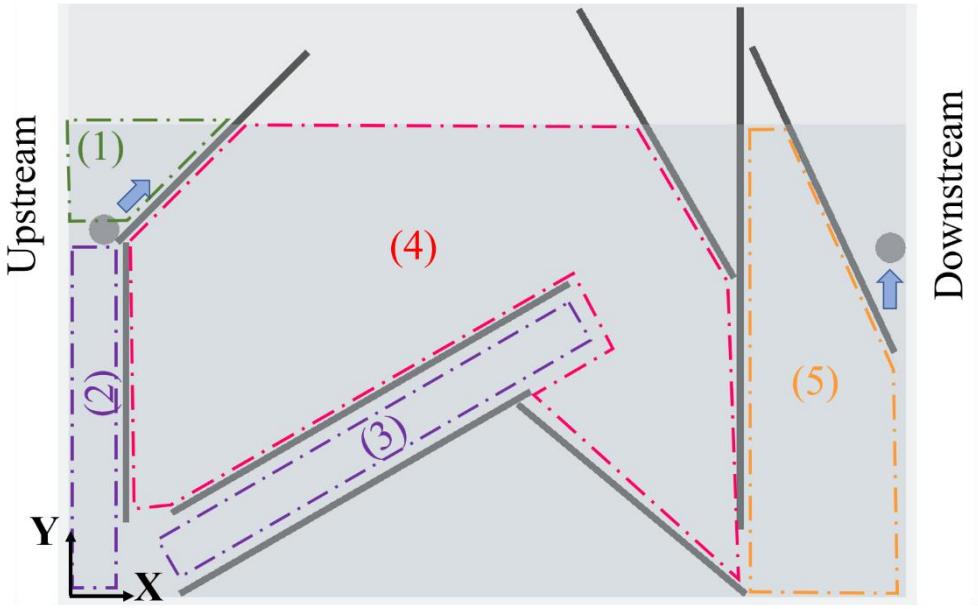

Figure 3.10: Schematic diagram of the final internal flow channel configuration.

3.1.6 Entrain-disengaging Zone

As the upstream region of the flow path, this zone was designed to ensure that dry, tangled feather samples were fully wetted and disentangled through dynamic immersion. The cross-sectional view of this area was trapezoidal, as shown in Figure 3.11 (a). The left side of the trapezoid aligned with the vertical wall of the water tank, while the right side was defined by a slanted partition forming a 45-degree angle with the X-axis.

doi:10.6342/NTU202404295

The inlet pipe was positioned 10 cm below the water surface, directing a series of jets at a 45° angle towards the water surface along the slanted partition, as shown in Figure 3.11 (a). The strong jets drove the fluid, creating a trapezoidal free surface that moved from right to left, ultimately curling down against the left wall of the water tank, forming a counterclockwise vortex, as illustrated in Figure 3.11 (a). After the tangled dry feather mixed sample, as shown in Figure 3.11(a), were placed to the surface of this zone, they were influenced by the surface flow field, as depicted in Figure 3.5(d). Coupled with the low surface tension characteristics of the solution, the feathers rapidly became dynamically wetted and were then drawn into the strong counterclockwise vortex below the water surface, as shown in Figure 3.11 (b). During this downward curling process, the tangled feather bundles experienced reverse pulling forces due to surface tension and the descending flow, leading to gradual disengaging.

We designed this rotational flow field to drive the movement of feathers, achieving a similar effect to the stirring of the solution described in Section 2.1 to accelerate the complete wetting of feather samples. Eventually, as the feathers followed the flow field and moved toward the lower side of the trapezoidal area, as shown in the red boxed area in Figure 3.11. Here, some feather samples exited the area through outflow A, as shown in Figure 3.11(a-A), which was a 1.5 cm wide gap along the water tank wall. Meanwhile, the remaining feather samples continued to swirl and roll back into the vortex via original

doi:10.6342/NTU202404295

flow, as indicated in Figure 3.11(a-B).

To further loosen the tangled feather clusters, we intentionally placed the exit of this area very close to the inlet pipe. We adjusted the spacing of the exit to be much smaller than the characteristic lengths of the feather clusters, which range from 4 to 15 cm. This setup ensured that when the tangled feather clusters approached the exit while following the rotating flow field, they would not be directly discharged. Instead, they would be subjected to the forces from both outflow and original flow, as well as the jet flow, creating flow forces in two different directions. This interaction would create tearing force and gradually loosen the clusters, separating them into individual feathers that are no longer entangled. The loosening effect, viewed from the x-direction into this area, is shown in Figure 3.11 (c).

It is worth mentioning that we chose to drive the surface flow below the liquid surface and indirectly wet the feathers at the liquid surface rather than having the jets directly act on the dry feathers at the surface. This approach aims to avoid incomplete wetting of the dry feathers, as described in Chapter 2.1, and excessive bubble formation, as described in Chapter 2.2. Additionally, the final design of this area was determined through trial and error with different sizes and shapes. The use of a narrower trapezoidal space was chosen to generate a sufficiently strong rotational flow field while avoiding secondary flows, which seems to enhance the feather disengaging mechanism. The

doi:10.6342/NTU202404295

narrow exit design also helps to block the discharge of large feather clusters and increases the time the feather clusters were subjected to the flow field for loosening and separation, achieving a better feather disengaging and individualization effect.

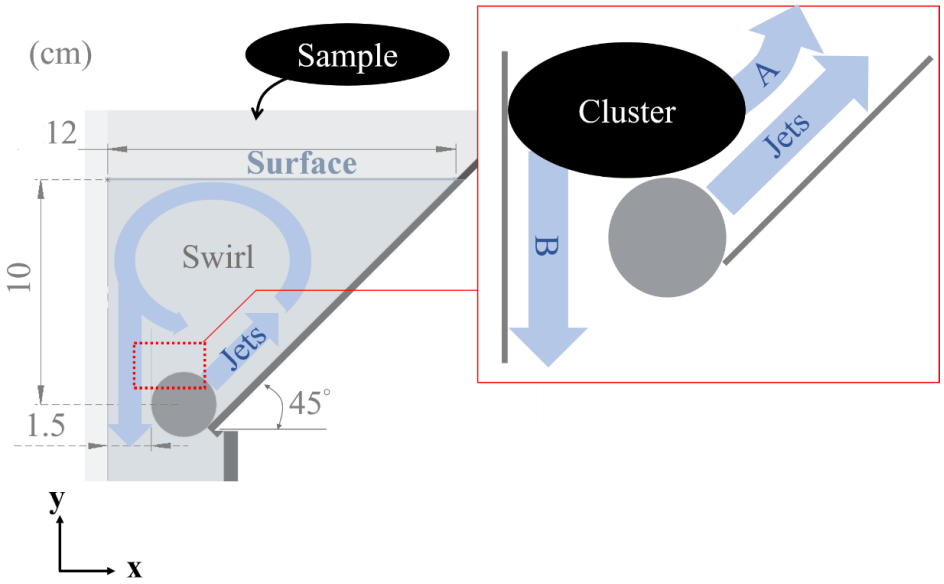

(a)

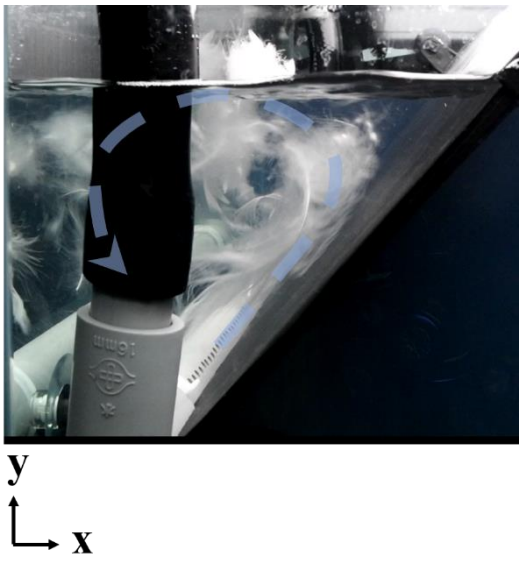

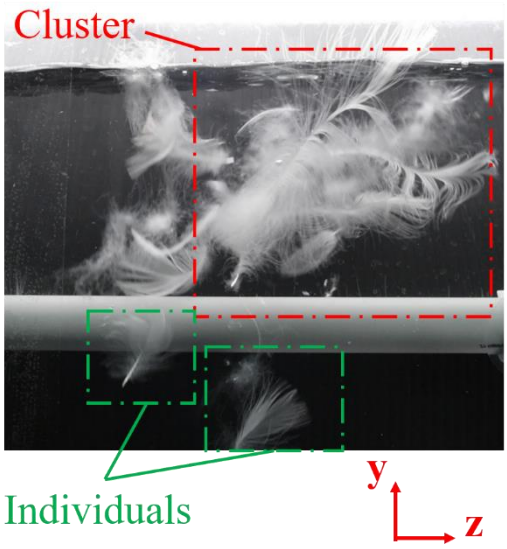

(b) (c)

Figure 3.11: (a) Schematic diagram of entrain-disengaging zone. (b) View of feather rotation motion in z-direction. (c) View of clusters disengaging effect in x-direction.

doi:10.6342/NTU202404295

3.1.7 Vertical transport channel

This area's goal was to efficiently transport the separated feather individuals to the bottom of the tank and channel them to the next zone. This ensured that the buoyancy difference between the big feathers and downs had enough space to act in the subsequent areas, facilitating their segregation effect. After leaving the entrain-disengaging zone, the feather individuals followed the flow into a vertical channel that was 25 cm long and positioned 4 cm from the left side wall of the tank, as shown in Figure 3.12 (I). Subsequently, they exited this transport zone moving in the positive x-direction at the bottom of the tank, as depicted in Figure 3.12 (II).

We designed this area with a narrower space to prevent the formation of secondary flow structures, like the large vortex in Figure 3.13 (a). At the same time, it ensured that the feathers experienced sufficient fluid force to overcome their buoyancy, preventing big feathers from becoming trapped in low-velocity areas near the top corners of the channel, as shown by the red boxed area in Figure 3.13(b), which could decreased transportation efficiency.

doi:10.6342/NTU202404295

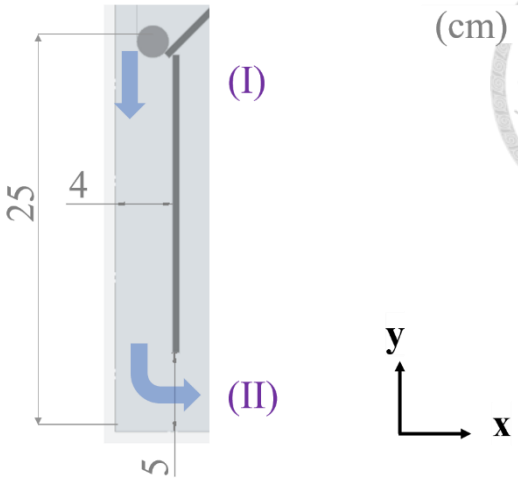

Figure 3.12: Schematic diagram of vertical transport channel.

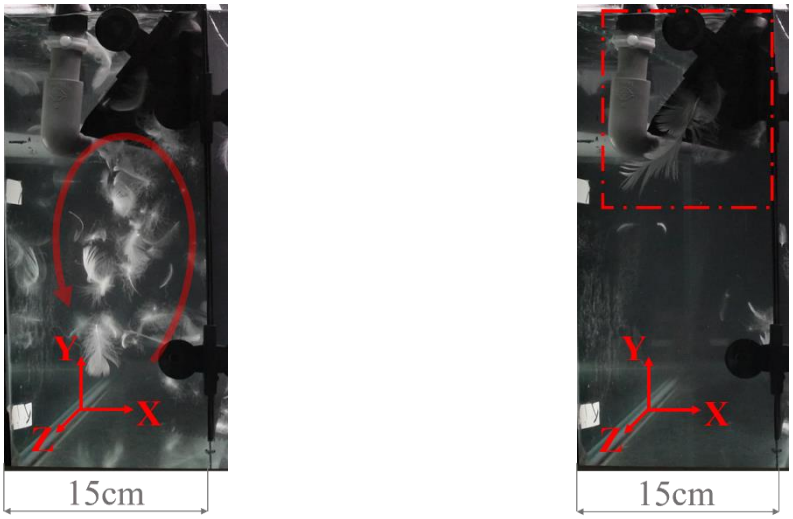

(a) (b)

Figure 3.13: (a) Vortex within the vertical channel；
(b) Big feathers with higher buoyancy were trapped in the upper part of the channel.

3.1.8 Slant transport channel

The purpose of the slant channel was to ensure that when feathers entered the intended separation zone, the fluid dynamics they experienced were as orthogonal as possible to their buoyancy, to avoid influencing the buoyancy segregation effect.

doi:10.6342/NTU202404295

Additionally, the channel used partitions to separate the transport and separation flow regions, preventing the flow fields in the two areas from interacting and creating flow structures which might be adverse for segregation.

The original flow field design did not include this slant channel, as shown in Figure 3.14 (a). We expected that the flow would directly exit the vertical channel, turn along the bottom of the tank in the +x-axis direction, and then flow through the separation zone and smoothly enter the right-side product collection zone, as indicated by the blue arrow in Figure 3.14 (a). Transportation and segregation were expected to occur simultaneously in this process.

However, the bottom transport flow field, due to its higher momentum, provided shear forces to the upper segregation zone, driving the separation zone fluid to move right as well. Additionally, as the transport flow field approached the right-side partition, it was blocked and created a local high-pressure point, causing some of the fluid to turn upward and form a large vortex in the segregation zone, as shown by the red arrows in Figure 3.14 (a). This vortex caused downs to move along with it and re-mix with the big feathers. The feathers and down caught in the large vortex tended to rotate continuously, making it difficult for them to escape through buoyancy and gravity, resulting in low segregation efficiency, as shown in Figure 3.14 (b)(c).

To make the interaction between the transport and separation flow fields less strong,

doi:10.6342/NTU202404295

we added a horizontal partition, as shown by the red line segment in Figure 3.15. to create a horizontal transport channel and separate the two areas. After trial and errors, the horizontal channel and segregation zone were connected with a 15 cm opening to reduce the influence of the transport flow field on the segregation flow field while allowing big feathers to enter the segregation zone smoothly. To compare the impact of this design on the segregation effect, we operated the apparatus with and without the horizontal channel until all feathers were no longer moved with the flow field, then turned off the pump for 10 minutes to allow the water to settle. We used the number of big feathers floating on the surface of the segregation and collection zones as reference values. The results showed that whether or not the partition was installed, about 20–30% of all floating big feathers entered the collection zone. Thus, adding the horizontal channel in the design seems to considerably decrease the time needed for segregation time, while having little impact on the segregation effect, as shown in Figure 3.15 (b)(c).

However, some feathers with higher buoyancy would apply more normal force at the channel's upper boundary. The resulting friction forces can even exceed the fluid forces from the transport flow, causing the big feathers to be trapped within the channel and unable to exit, as shown in Figure 3.15 (c) with the red-highlighted area and its enlarged view in Figure 3.15 (d). This can potentially lead to blockages.

doi:10.6342/NTU202404295

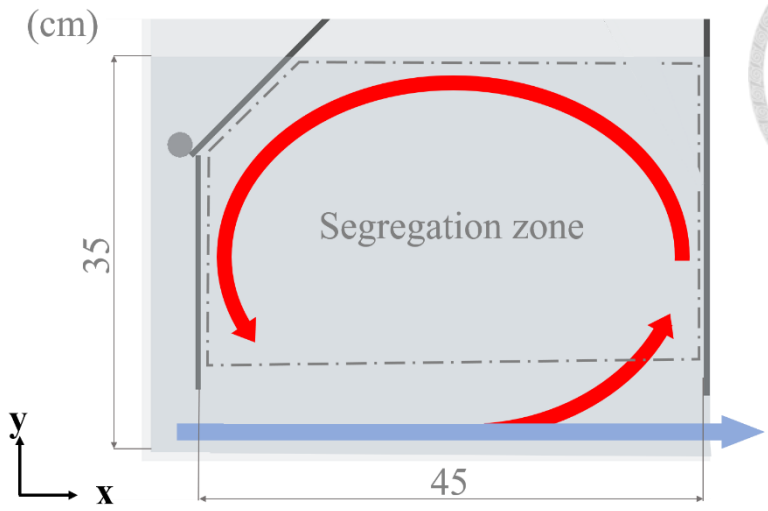

(a)

(b)

(c)

Figure 3.14: (a) Schematic diagram of flow field design without slant channel；Suspension of 1g mixed feather samples in the segregation zone after (b) 1 minute and (c) 5 minutes.

doi:10.6342/NTU202404295

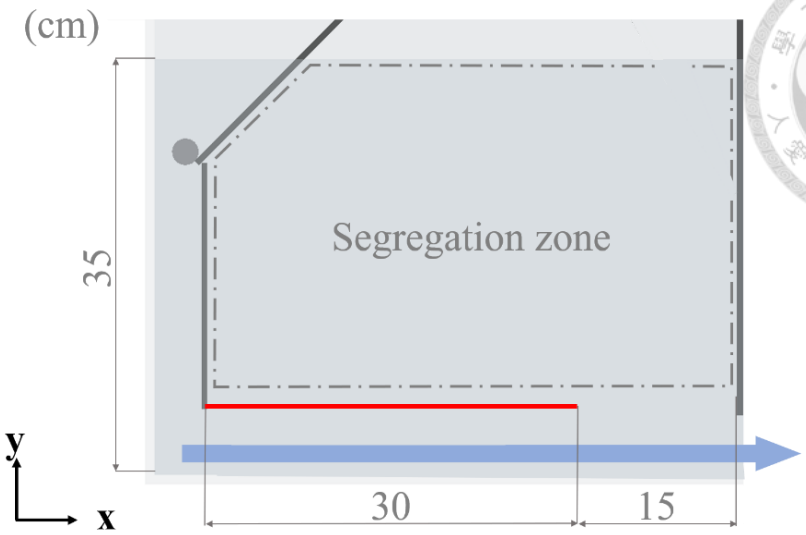

(a)

(b)

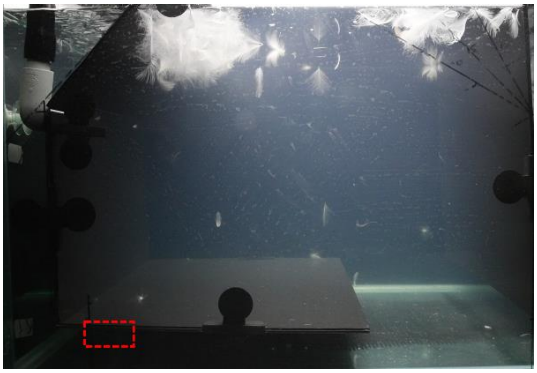

(c)

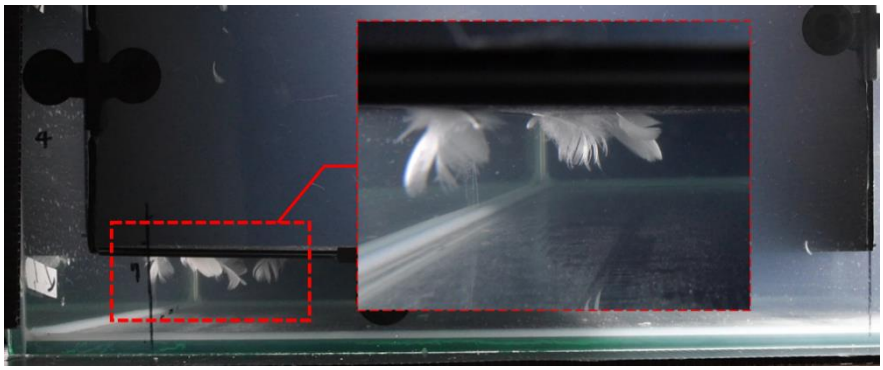

(d)

Figure 3.15: (a) Schematic diagram of flow field design with horizontal channel； Suspension of 1g mixed feather samples in the segregation zone after (b) 1 minute and (c) 5 minutes ；(d) Enlarged view of the trapped feather in the red-boxed area of (c).

doi:10.6342/NTU202404295

To reduce the friction force between big feathers with strong buoyancy and the upper plate, we adjusted the angle ϕ of the transport channel relative to the +X-axis, making it inclined towards the water surface. The channel length was kept at 30 cm, with an opening width of 15 cm connecting to the segregation zone, as shown in Figure 3.16. This adjustment aimed to decrease the normal force component of buoyancy perpendicular to the channel's upper plate and increase the buoyancy component parallel to the transport flow field. After trials, we found that when the angle $\phi > 30°$, nearly all big feathers with high buoyancy slid along the upper boundary of the channel in the direction of the flow field, as seen in Figure 3.17. Thus, it was confirmed that both mechanisms effectively address the issue of big feathers blocking the horizontal transport channel.

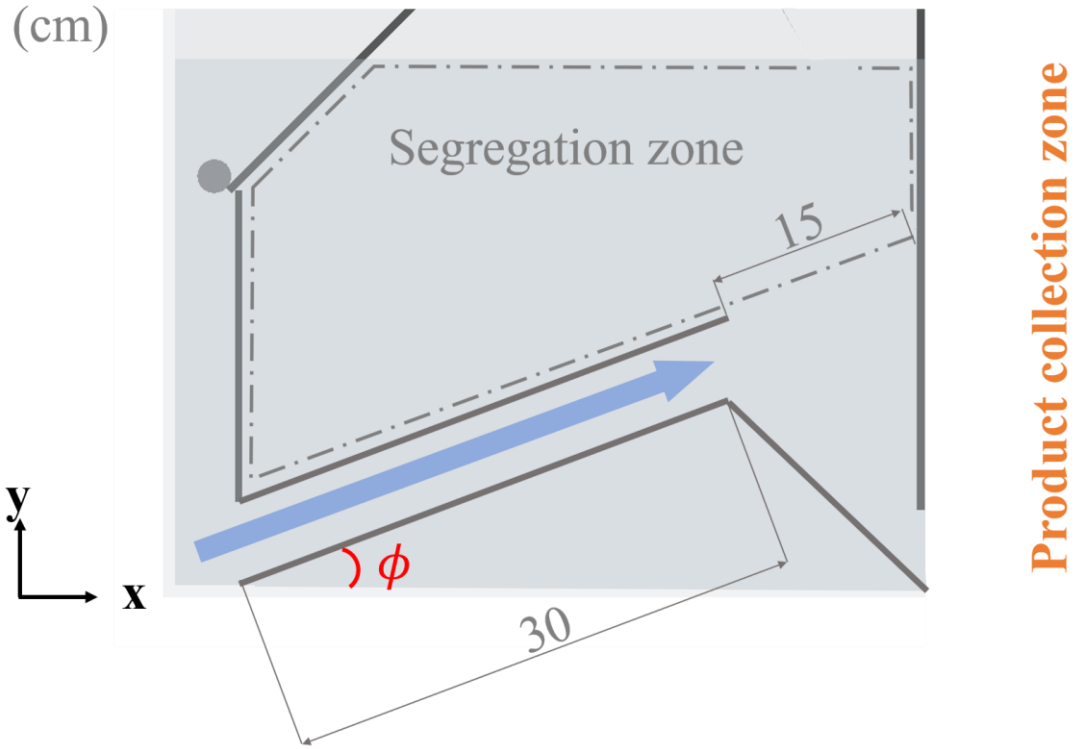

Figure 3.16: Schematic diagram of flow field design with slant channel.

doi:10.6342/NTU202404295

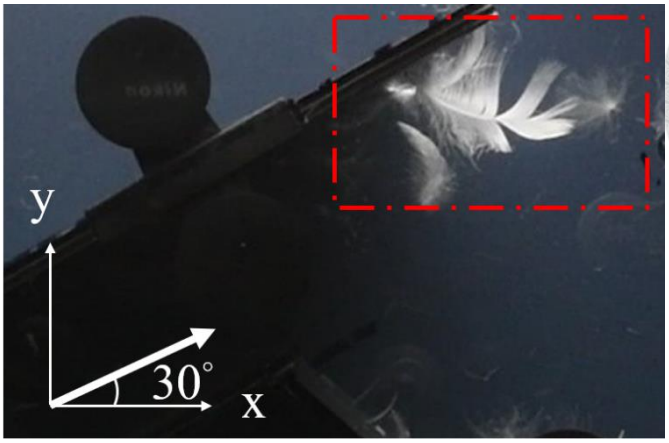

(a)

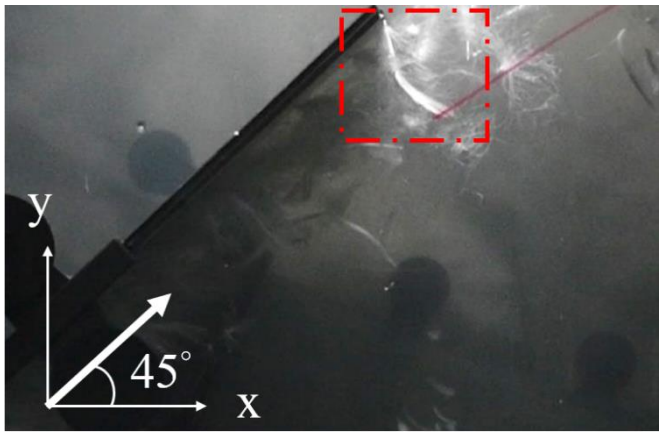

(b)

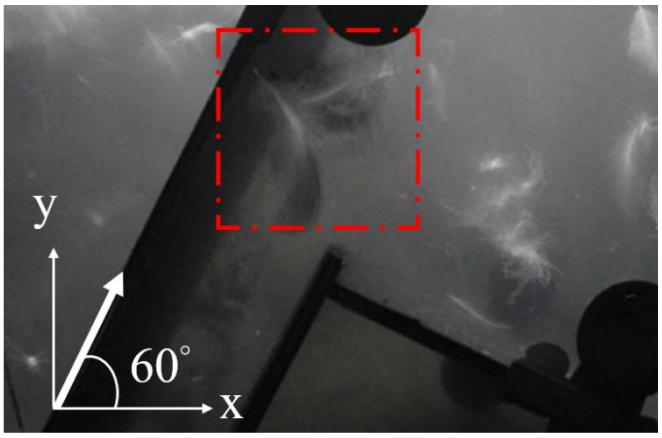

(c)

Figure 3.17: Big feathers slid along the upper boundary of the slant channel at the inclined angle ϕ = (a) 30°, (b) 45°, and (c) 60°.

doi:10.6342/NTU202404295

To verify the difference in transport efficiency between inclined and horizontal channels, we randomly selected 10 big feathers with a density below 1.0 g/cm³ in a wetted state as testing samples. After operating the apparatus for 5 minutes to stabilize the flow field, each test involved placing one sample into the tank and measuring whether it could pass through the transport channel within 30 seconds. Each sample was tested 3 times. The test results are shown in Figure 3.18. The first set of test images are shown in Figure 3.19. The results revealed a 90% chance of trapping big feathers in the horizontal channel, compared to a 0% chance at a 30° inclination. As a result, it was evident that the 30° inclined channel has significantly better transport efficiency.

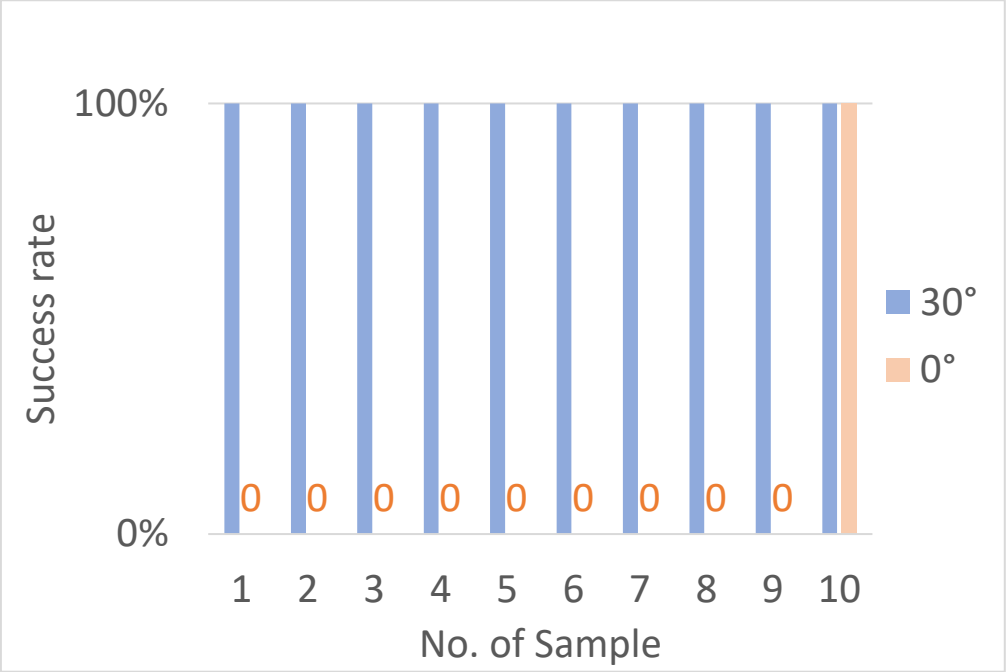

Figure 3.18: The results of the horizontal and slant channel transport efficiency tests.

doi:10.6342/NTU202404295

Inclined angle ϕ	Time (sec)	Image
0°	0	
	10	
	20	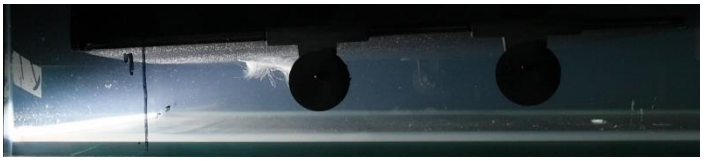
	30	
30°	0	
	10	
	20	
	30	

Figure 3.19: The images captured at 10-second intervals from 0 to 30 seconds after the sample reached the starting point in the first set of testing.

doi:10.6342/NTU202404295

Under this concept, we also attempted to increase the channel spacing to improve transport efficiency. However, excessively large channel spacing led to issues similar to the vortex formation observed in the vertical channel. Therefore, after evaluating the orthogonality between the direction of the flow exiting the channel and buoyancy and under acceptable conditions with minimal big feathers being stuck, the final decision was to set the channel at a 30° angle relative to the +X-axis, as shown in Figure 3.20.

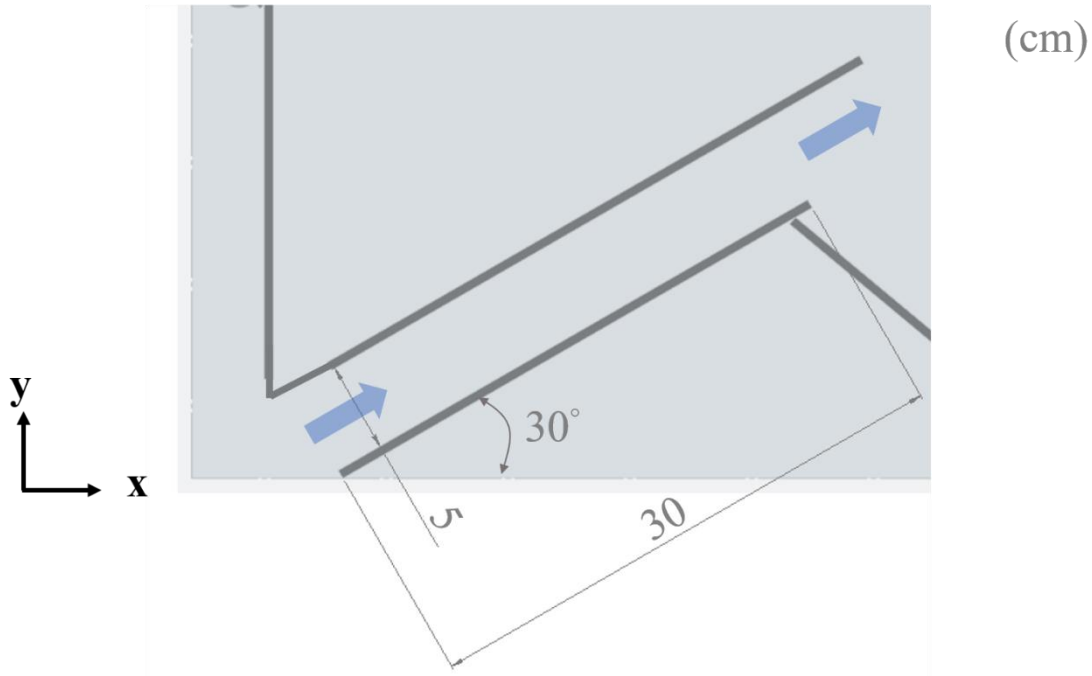

Figure 3.20: Schematic diagram of the final inclination angle of the slant channel.

3.1.9 Segregation zone

After exiting the slant transport channel, the fluid's inertia largely maintained the original flow direction. When the flow reached the right-side partition wall, as indicated by the red solid line in Figure 3.21, it branched into two directions, similar to an oblique

doi:10.6342/NTU202404295

stagnation point flow. The main flow, shown by the orange arrow in Figure 3.21, was driven by the suction pipe in the downstream collection zone. It turned toward the bottom of the tank and flowed out of the segregation zone through a 5-cm-wide exit at the tank's bottom. The secondary flow, as shown by the blue arrow in Figure 3.21, turned towards the liquid surface and then proceeded in the -X direction, forming a secondary flow that passed through the area depicted in Figure 3.21 (II).

After the feather samples exited the slant channel and entered the segregation zone, the downs, which had weaker buoyancy, moved primarily in the -Y direction. They reached the downs transport area, as shown in Figure 3.21(a-I), and were trapped by the induced secondary flow vortex, as shown by the orange dashed line box in Figure 3.21(b), eventually flowing out into the collection area；Big feathers, which had stronger buoyancy, floated upwards after leaving the inclined channel, overcoming the primary flow’s force. They followed the upward secondary flow through the opening between the slant channel and segregation zone, eventually reaching the liquid surface. These big feathers then moved with the weak secondary flow to the big feather collection zone, as shown in Figure 3.21(a-II), and continued to float there, making them easy to collect, as shown by the blue dashed line box in Figure 3.21(b)

Based on the above description, we aimed to use the differing buoyancy and gravity of big feathers and downs to separate them. The preliminary objectives of transport and

doi:10.6342/NTU202404295

collecting using the flow field were achieved. Additionally, during the observation of the separation process, we found that the two types of feathers, when moved by the flow field, changed their movement trends based on the resultant forces they experienced upon collision with the wall or through the coupling interactions within the flow field. We speculated that slight differences in movement might have arisen from varying collision angles with the wall. The previously described experiments only used a $\theta = 90°$ setup. To test the effects of different collision angles, we used the lower boundary of the inclined channel extending towards the end-wall intersection was used as the pivot point. From this pivot, the collision board was placed and extended to the liquid surface, as shown by the solid red line in Figure 3.21. By adjusting the angle of this collision board, we aimed to investigate its relationship with feather segregation efficiency.

It is worth noting that some downs still entered the collection area for big feathers due to collisions and the flow field near the wall, leading to lower efficiency in downstream downs collection. To address this issue, we created a 3 cm gap at the entrance of the slant channel, as shown in Figure 3.21 (III). After trial and error, we observed that the velocity difference between the slant transport channel and the segregation zone created a slight suction flow at this gap, which slightly altered the secondary flow structure within the segregation zone. This modification, when combined with the

doi:10.6342/NTU202404295

gravitational effect on the downs, provided an opportunity for the downs to be redirected back into the channel for re-sorting, as illustrated in Figure 3.22.

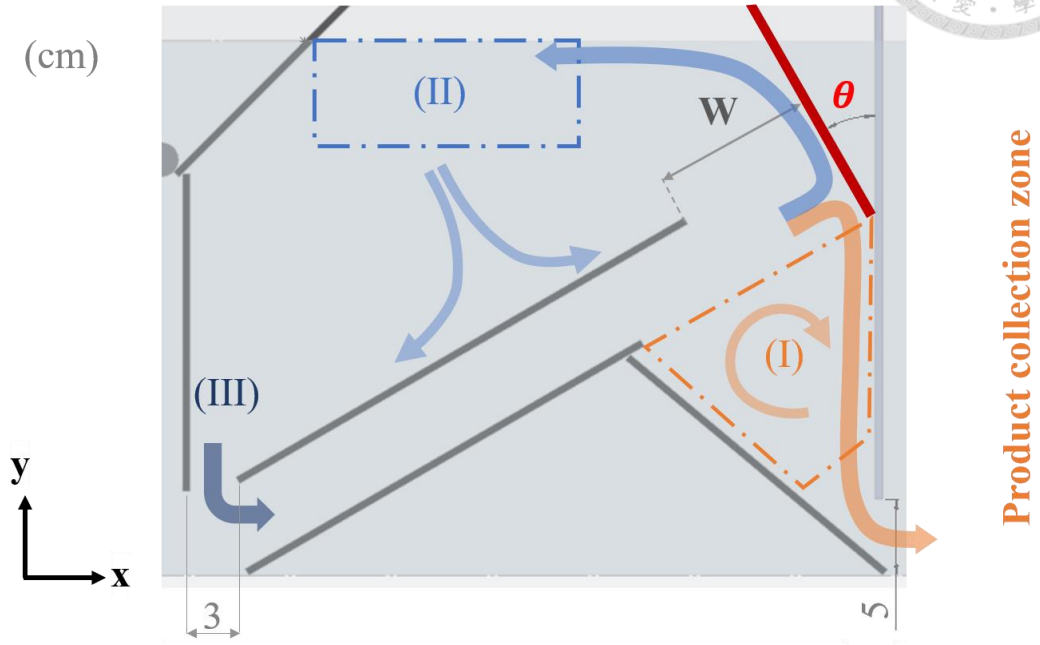

(a)

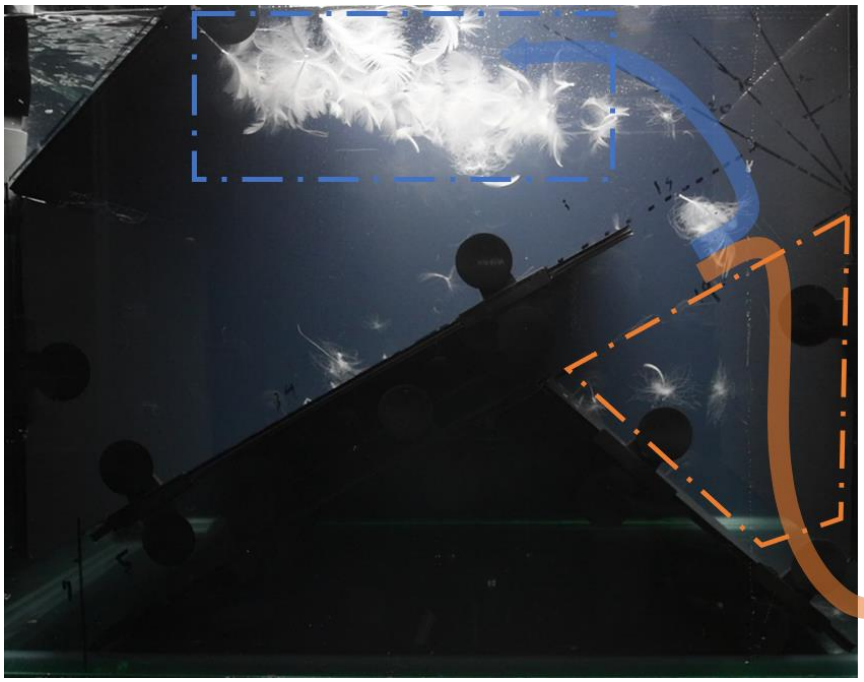

(b)

Figure 3.21: (a) Schematic diagram of the segregation zone；
(b) real image of the segregation zone

doi:10.6342/NTU202404295

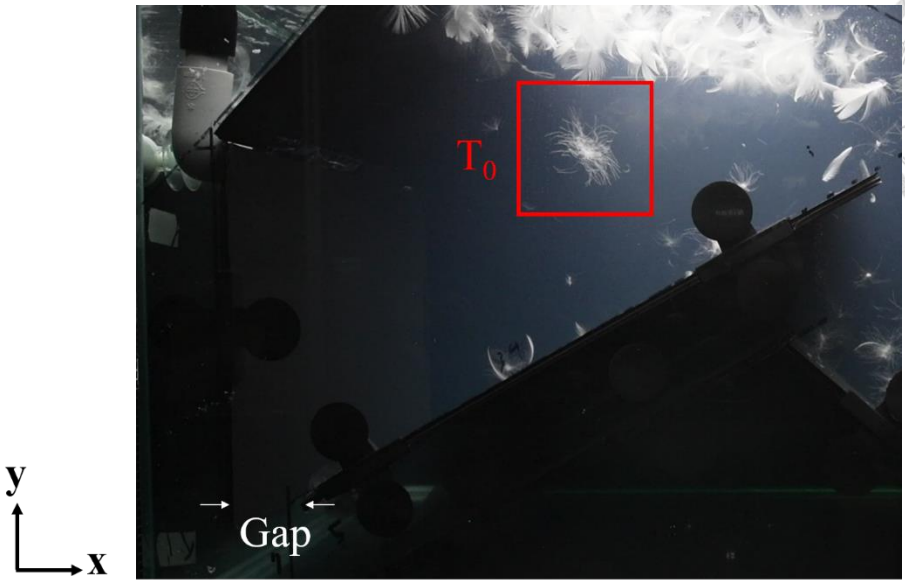

(a)

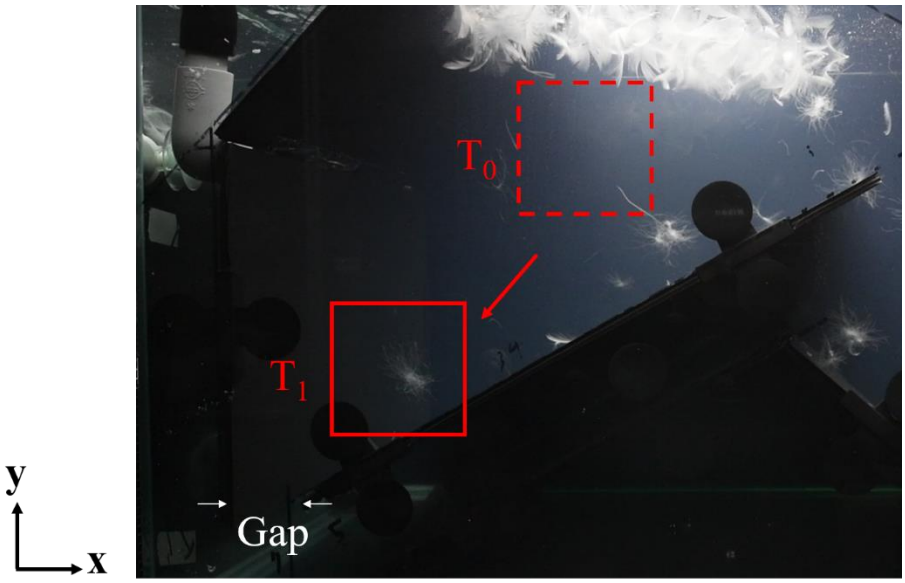

(b)

Figure 3.22: The 3 cm gap at the entrance of the slant channel allowed the downs that entered the collection area for big feathers to gradually return to the slant transport channel after (a) T_0 ; (b) $T_1 = T_0 + 40$sec.

doi:10.6342/NTU202404295

3.1.10 Collection zone

The outlet pipe drove the flow field that entrained all feathers entering this area from the bottom of the tank toward the liquid surface. Ultimately, these product feathers were intercepted and adhered to the strainer, as shown in Figure 3.23. Once the experimental process concluded, we removed the strainer from the tank and gathered the product feathers. The actual operational image is shown in Figure 3.23.

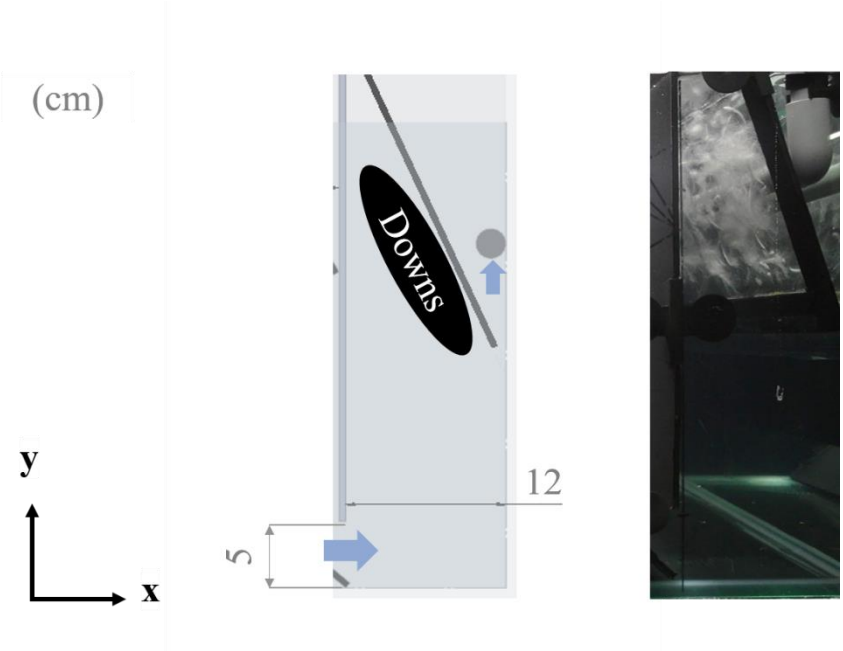

Figure 3.23: Schematic diagram and actual operational image of the collection zone

3.1.11 Verification of segregation mechanism

To validate the influence of buoyancy on our apparatus's segregation mechanism, we conducted tests with fully wetted large feathers of varying densities. We used static buoyancy tests to select equal numbers of large floating feathers from each density range

doi:10.6342/NTU202404295

to serve as samples. We then individually tested these feathers in the apparatus to evaluate the probability of their upward movement after exiting the slant channel. A random sample of 20 large feathers was taken from each density range. Each sample was tested five times to calculate its probability of floating under operational conditions. The results of the average floating probability and standard deviation for the 20 samples in each density range are shown in Figure 3.14.

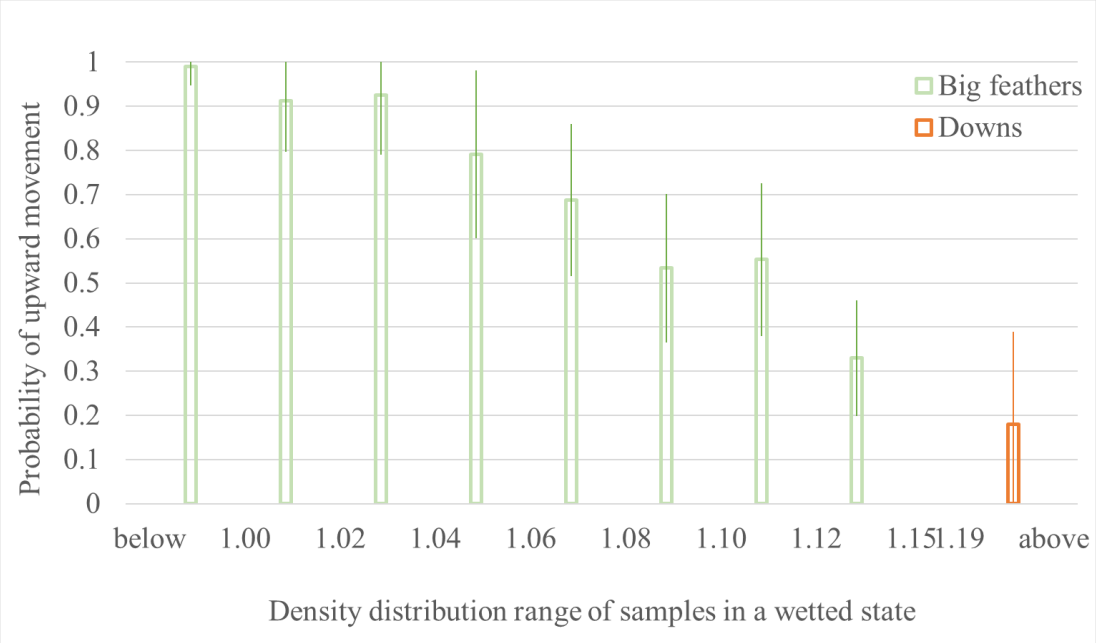

Figure 3.24: Probability of floating after equipment operation for wetted samples across different density ranges.

The results showed that as the density of the fully wetted large feathers increased, the average probability of floating gradually decreased. Moreover, the standard deviation started at 0.04 for densities below 1.0, increased to 0.17 for densities between 1.10 and 1.12, and then decreased to 0.13 for the density range of 1.12 to 1.15. We speculated that

doi:10.6342/NTU202404295

the observed trend occurs because buoyancy primarily governs the motion of low-density large feathers, making their movement more stable. As the density of the feathers increased, the influence of fluid dynamics began to outweigh the effects of buoyancy. This shift caused the feathers' size and appearance to increasingly influence their movement. Once the forces of gravity and fluid dynamics significantly surpassed the effects of buoyancy, the feather movement trend became more stable.

It is worth noting that the results indicate that down feathers had an approximate 20% probability of floating, thus supporting the re-sorting mechanism for downs described in section0 was a necessary design.

3.2 Experiment on the Effect of Collision Board Angle on Sorting

For the flow field setup discussed in the section 3.1.5, the main objective of this experiment was to investigate the effect of different collision board angles (θ) on feather sorting results.

Before starting the collision plate experiments, we first confirmed that the final working fluid formulation described in 0 was effective in fully wetting the dry mixed feathers, thereby avoiding any impact on the separation results. To do this, we conducted preliminary tests with two different surfactant concentrations: 0.5 g per liter of brine and

doi:10.6342/NTU202404295

3 g per liter of brine, each with the collision board set at θ = 90°. We performed five tests for each setup and compared the results with the separation mechanism validation described in section 0. to make sure that the final working fluid formulation would still work in this apparatus. Only then did we move on to the main experiments.

Subsequently, the main experiments were conducted with the collision plate angles set to θ = 90°, 60°, and 30°, with each configuration tested five times using the same procedure. Each test used 1 g of dry feather mixtures as the testing sample, as described in Chapter 3. The working fluid was maintained at a temperature of 25 ± 2°C and a density of 1.1 ± 0.002 cm^3, as described in section 2.2. The flow rate was fixed at 1302 L/h, as described in section 0. Except for the collision plate angle θ, all other flow channels were set according to the final configuration described in section 3.1.5.

The results of each tests were divided into three groups for collection the product collection area, as shown in Figure 3.25(I)；the waste feather collection area, as shown in Figure 3.25 (II)；and all other areas not included in the above two zones. After collection, the samples were sent to the feather supplier to analyze of the proportions of composition in each area.

doi:10.6342/NTU202404295

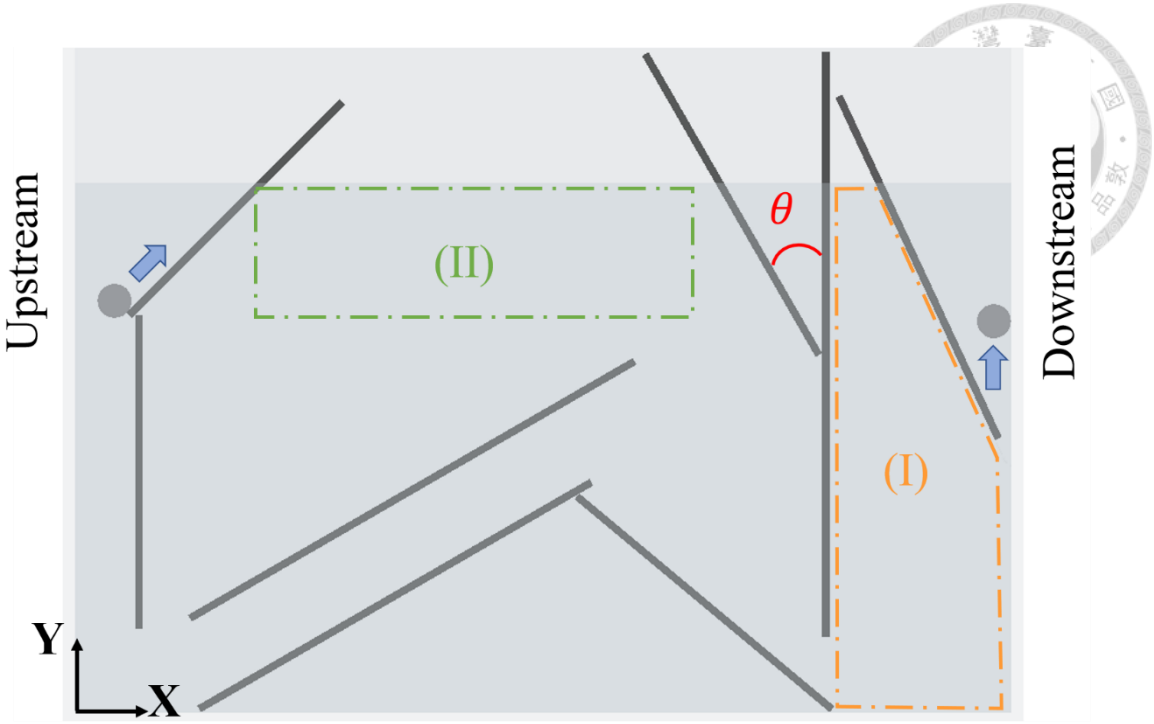

Figure 3.25: Schematic diagram of the collision board angle experiment
(I) product collection area；
(II) waste feather collection area.

The experimental image used to illustrate the experimental procedure is shown in Figure 3.26, while shows the main experimental procedure, with details including:

3.2.1 Pre-experiment processing

1. Measure the density, temperature, and water level of the liquid.

2. Adjust the angle of the collision plate and ensure that all other flow paths are in the correct position.

3. Set up all observation, lighting, and recording equipment.

4. Randomly take 1g of mixed dry feathers from the reservoir and divide it into two

doi:10.6342/NTU202404295

portions, placing each in separate dry plastic cups.

5. Start the motor and run the equipment for 5 minutes at the experimental flow rate, assuming the flow field reaches a near-steady state, so that each experiment starts under similar flow field conditions.

6. Double-check all settings to ensure they are correct before beginning the experiment.

3.2.2 Main experimental procedure

1. Turn on all lighting and recording equipment.

2. Start the timer for 10 minutes and simultaneously place 0.5g of mixed dry feathers on the surface of the immersion and loosening zone in the water tank.

3. After one minute, add the remaining 0.5g of mixed dry feathers at the same location.

4. After the remaining 9 minutes have elapsed, end the experiment.

3.2.3 Post-experiment processing

1. Turn off all lighting and recording equipment.

2. Shut down the motor.

3. Close the connection between the segregation zone and the collection zone.

4. Carefully remove the filter from the collection zone and collect all feathers from the finished product collection area, as shown in Figure 3.26 (I). Place them in a designated

doi:10.6342/NTU202404295

clean water basin and remove all feather materials.

5. Gently scoop out and collect feathers from the waste feather collection area, as shown in Figure 3.26 (II). Place them in a designated clean water basin and remove all feather materials.

6. Collect all remaining feathers from the water tank, as shown in Figure 3.26 (III), place them in a designated clean water basin, and remove all feather materials.

7. Rinse the feathers from all three areas with clean water three times. Use colored filter paper (coffee filters) to filter and collect all feather materials separately.

8. Place the feathers wrapped in filter paper in a cool room for 24 hours to dry.

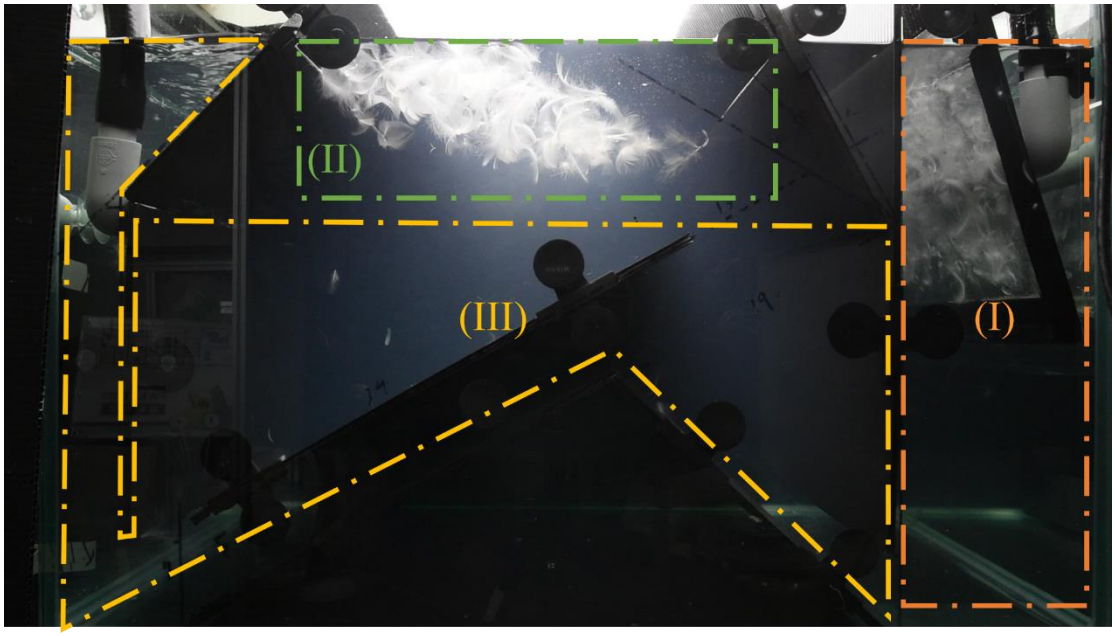

Figure 3.26: Real image after the experiment, included (I) collection area；(II) waste feather collection area；(III) other area.

doi:10.6342/NTU202404295

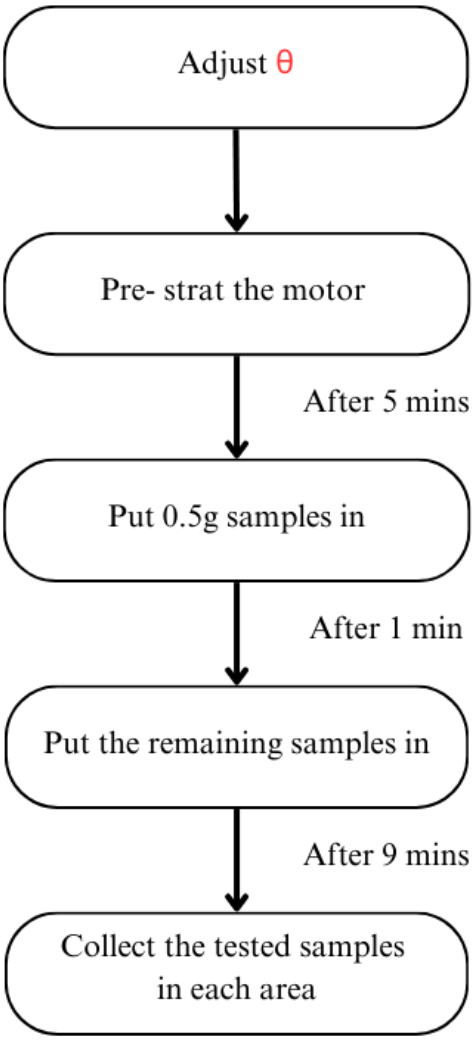

Figure 3.27: Experimental procedures for the collision board angle experiment and the surfactant concentrations experiment

3.3 Experiment Results and Discussion

The experimental results were initially analyzed using the feather separation quality measurement commonly employed by feather suppliers. This approach calculates the weight percentage of downs relative to the total weight of all samples in the corresponding calculation area, represented as $wt\%_D$.

doi:10.6342/NTU202404295

We initially anticipated that if the surfactant concentration was insufficient to fully wet the downs, bubbles might form on them, leading to enhanced buoyancy and resulting in their entry into the waste feather collection area. Therefore, we compared the average weight percentage of down feathers in the waste feather collection area across five experiments for two different surfactant concentrations, as shown in Table 3:

Table 3: The average weight percentage of downs in the waste collection area under different surfactant concentrations, based on five repeated testing for each setup.

Surfactant concentration (g/L)	0.5	3.0
Average of $wt\%_D$ (%)	9.76	2.32
STD	2.30	1.01

The results show that the lower surfactant concentration in the working fluid resulted in a significantly higher perception of down feathers in the waste feather collection area, which was in line with our presumption. In contrast, the higher surfactant concentration setup had only 2.3% of downs in the waste feather collection area, confirming that this final formulation of working fluid provided an adequate level of wettability.

However, the experimental data calculated for the product collection area, as shown in Table 4, indicated that the setup with a lower surfactant concentration had a significantly higher percentage of downs in the product collection area. This result contradicted the earlier findings. We speculated that this discrepancy might be due to the

doi:10.6342/NTU202404295

calculation method, which uses the total feather weight in the area and the weight percentage of a single type of feather. This method did not consider that the average weights of different types of feathers might be different, and the weight differences within the same sample may be substantial, which might lead to a distorted calculation.

Table 4: The average weight percentage of downs in the product collection area under different surfactant concentrations, based on five repeated testing for each setup.

Surfactant concentration (g/L)	0.5	3.0
Average of $wt\%_D$ (%)	47.97	41.84
STD	2.16	5.63

Therefore, we measured the weight and count of large feathers, small feathers, and downs in their dry state from all experimental groups and calculated their average weights. These statistical samples consisted of 20 g of randomly selected mixed dry feathers, which included 4,662 downs, 3,434 small feathers, and 895 large feathers. Table 5 shows the average weights of the three feather types. The results indicated that the average weights of downs and small feathers were relatively close, while the large feathers were approximately 10 times heavier than the other types. This confirmed our speculation.

doi:10.6342/NTU202404295

Table 5: The average weight of each type of feather in the total feather sample used during the experiment.

	Big feather	Down	Small feather
Average weight (mg)	10.374	1.185	1.560
STD	0.783	0.159	0.183

To avoid the calculation flaws mentioned earlier, we changed our analysis method to calculating the percentage of each specific feather type within the designated areas in relation to its initial total count, represented as Ct%. Table 6 shows the results of re-evaluating the surfactant experiments in the waste feather collection zone and the product collection zone using this calculation method. The results indicate that with the higher surfactant concentration setup, an average of 87% of the down feathers entered the product collection zone, while with the lower surfactant concentration setup, only 72% did.

Subsequently, we compared this result with the downs flotation probabilities measured in section0, as shown in Figure 3.28. The results show that, under the lower surfactant concentration setup, the percentage of downs in the waste feather collection zone was close to the flotation probability of themselves. Thus, it can be inferred that most of the downs entering this zone were floating and unable to leave, which in line with our initial speculation regarding how the wettability of the working fluid affects the sorting performance.

doi:10.6342/NTU202404295

Table 6: The average count percentage of downs in the waste collection area and product collection area under different surfactant concentrations, based on five repeated testing for each setup.

Surfactant concentration (g/L)		Waste collection area	Product collection area
0.5	Average of $Ct\%_D$ (%)	16.35	72.02
	STD	2.42	4.92
3.0	Average of $Ct\%_D$ (%)	6.1	87.03
	STD	3.05	2.33

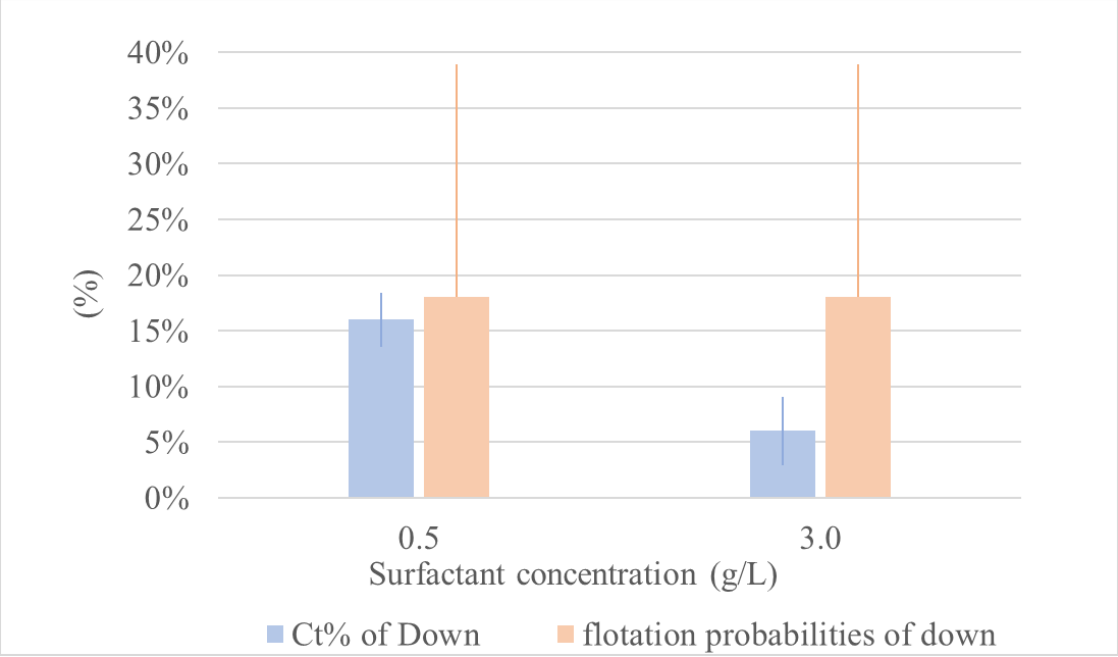

Figure 3.28: Comparison of $Ct\%_d$ in the waste feather zone and down feather flotation probability.

We then expressed the collision board angle testing results in terms of average percentage values, as shown in Table 7 and Figure 3.29. The results show that as the angle of the collision board decreased from 90° to 30°, the percentage of each feather type entering the product collection area increased as expected. However, while the percentage

doi:10.6342/NTU202404295

of downs only slightly increased from 87% to 90%, the percentage of big feathers increased from 22.5% to 33.4%. The rate of increase for big feathers was approximately three times greater than that for downs. Therefore, it could be inferred that the flow field changes near the wall's turning point had a more significant impact on the movement of big feathers compared to downs.

Furthermore, all experimental setups showed approximately 10% of down feathers remaining in the other areas. This indicated that the re-sorting design for downs, as described in section 0, required a longer operational time to improve its effectiveness. Additionally, the other areas contained only a very small number of big feathers, most of which were observed as extra-large feathers remaining in the immersion and loosening zones and failing to exit. However, similar extra-large feathers were also found in the collection and waste areas. This suggested that these extra-large feathers were less likely to leave the immersion zone compared to other types of feathers. Nevertheless, with the addition of more feathers causing collisions, and when the feathers themselves were positioned more parallel to the vertical walls of the tank, there was still a chance for them to exit this zone.

doi:10.6342/NTU202404295

Table 7: Results of the collision plate angle experiment showed as the count percentage of big feather ($Ct\%_{BF}$) and down ($Ct\%_{D}$) in product collection area. based on five repeated testing for each setup.

Collision board angle θ°		$Ct\%_{BF}$ in product collection area	$Ct\%_{D}$ in product collection area
90°	Average (%)	22.49	87.02
	STD	7.06	2.33
60°	Average (%)	26.02	88.18
	STD	6.01	3.15
30°	Average (%)	33.38	90.54
	STD	5.47	2.57

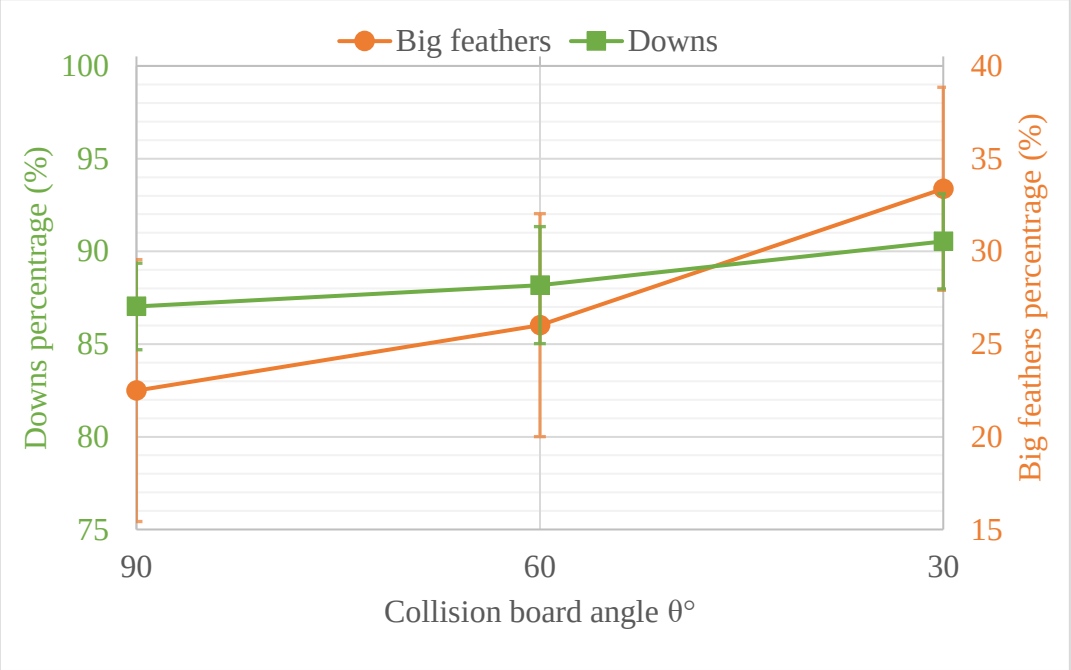

Figure 3.29: Results of the collision plate angle experiment showed as the count percentage of big feather (Ct%BF) and down (Ct%D) in product collection area. based on five repeated testing for each setup.

doi:10.6342/NTU202404295

Considering the loss of the downs due to sorting failures and the purity of the downs in the final collected product, we determined that the 90° collision board angle was the most suitable design for this apparatus. The experimental results under this setup indicated that within the planned 10-minute operation time for 1g dry feather mixtures, the apparatus maintained an 87% collection rate for downs while successfully separated 77% of the big feathers. Figure 3.30 shows the images of big feathers and downs that were collected in the product collection area, the waste feather area, and the other area after sorting 1 gram of dry mixed feather samples using this setup.

(a)

(b)

doi:10.6342/NTU202404295

(c)

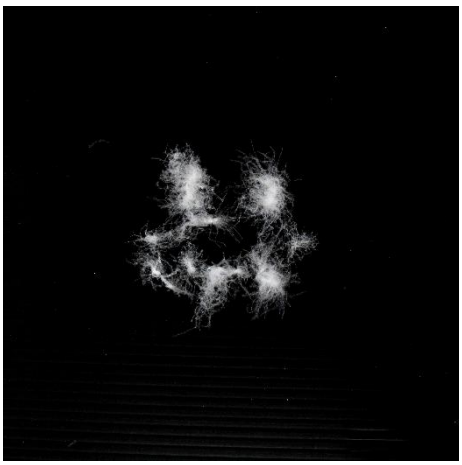

Downs	Big feathers

Figure 3.30: The different types of feathers collected in
(a) product collection area；(b) waste feather area；(c) other area.

doi:10.6342/NTU202404295

Chapter 4 Conclusion

This research provides a new immersion sorting method that differs from conventional feather sorting method and has preliminarily validated its feasibility, potentially leading to more efficient and cost-effective production processes. we successfully developed a small-scale model of an immersed flow field sorting system capable of running all stages of the sorting process, such as wetting, unraveling, transport, separation, and collection, without interruption. This system significantly separates big feathers from the dry feather mixture, thereby increasing the proportion of downs in the final product. By adjusting the formulation of the working fluid, such as adding sodium chloride and surfactants, we were able to enhance the buoyancy and wetting ability of the fluid on the feather mixtures, thus improving the sorting efficiency of the system. The entrain-disengaging zone, vertical transport channel, and slant transport channel, along with other flow channels and zones built into the experimental apparatus, play a crucial role in achieving the desired sorting results. The experimental results showed that the flow field, when coupled with the fluid property, could efficiently separate different types of feathers based on their buoyancy differences.

Future work could focus on testing different flow field parameters to further optimize the flow field design and explore the application of this system on a larger scale.

doi:10.6342/NTU202404295

Furthermore, we could engage in a deeper conversation about the techniques for gathering the finished goods. The integration of this sorting mechanism into existing industrial processes to simplify feather processing in the textile industry can also be explored.

doi:10.6342/NTU202404295

REFERENCE

[1] M. Thompson. "Everything You Need To Know About Feathers." https://academy.allaboutbirds.org/feathers-article/ (accessed.

[2] L. PACIFIC FEATHER CO. "Feather & Down Knowledge." https://www.pacificfeather.com.tw/en/downs_feathers (accessed.

[3] "HOP LION FEATHER WORKS CORP. Knowledge of Down & Feather," ed.

[4] " FEATHER INDUSTRIES. (n.d.). The Process." https://featherind.com/down-information/the-process/ (accessed July 21.

[5] T.-L. Yeh, "Experimental investigation of separation and collection mechanisms for feathers," Master, mechanical engineering, National Taiwan University, National Taiwan University, 2021.

[6] M. R. Arie, "The Structure and Functions of the Contour Feathers of Water Birds Revisited," in *Birds*, M. Heimo Ed. Rijeka: IntechOpen, 2023, p. Ch. 7.

[7] A. M. Rijke and W. A. Jesser, "The Water Penetration and Repellency of Feathers Revisited," *The Condor,* vol. 113, no. 2, pp. 245-254, 2011, doi: 10.1525/cond.2011.100113.

[8] A. M. Rijke, "Wettability and Phylogenetic Development of Feather Structure in Water Birds," *Journal of Experimental Biology,* vol. 52, no. 2, pp. 469-479, 1970, doi: 10.1242/jeb.52.2.469.

[9] P. L. Walker, E. E. Petersen, and C. C. Wright, "Surface Active Agent Phenomena in Dust Abatement," *Industrial & Engineering Chemistry,* vol. 44, no. 10, pp. 2389-2393, 1952/10/01 1952, doi: 10.1021/ie50514a032.

[10] R. Stephenson and C. A. Andrews, "The effect of water surface tension on feather wettability in aquatic birds," *Canadian Journal of Zoology,* vol. 75, no. 2, pp. 288-294, 1997, doi: 10.1139/z97-036.

[11] R. Sunga. "The Complete Sodium Chloride Density-Concentration Table Calculator." https://www.handymath.com/cgi-bin/nacltble.cgi?submit=Entry (accessed.

doi:10.6342/NTU202404295